Electronic Research Archive

http://www.aimspress.com/journal/era

ERA, 32(12): 6503–6534.
DOI: 10.3934/era.2024304
Received: 17 October 2024
Revised: 15 November 2024
Accepted: 22 November 2024
Published: 02 December 2024

Research article

Hopf bifurcation induced by fear: A Leslie-Gower reaction-diffusion predator-prey model

Jiani Jin[1,2], **Haokun Qi**[1] **and Bing Liu**[1,*]

[1] School of Mathematics, Anshan Normal University, Anshan Liaoning 114007, China

[2] School of Mathematics, Liaoning Normal University, Dalian Liaoning 116029, China

* **Correspondence:** Email: liubing529@126.com.

Abstract: The aim of this paper was to explore the impact of fear on the dynamics of prey and predator species. Specifically, we investigated a reaction-diffusion predator-prey model in which the prey was subjected to Beddington-DeAngelis type and the predator was subjected to modified Leslie-Gower type. First, we analyzed the existence and stability of equilibria of the nonspatial model, and further investigated the global stability and Hopf bifurcation at the unique positive equilibrium point. For the spatial model, we studied the local and global stability of the unique constant positive steady state solution and captured the existence of Turing instability, which depended on the diffusion rate ratio between the two species. Then, we demonstrated the existence of Hopf bifurcations and discussed the direction and stability of spatially homogeneous and inhomogeneous periodic solutions. Finally, the impact of fear and spatial diffusion on the dynamics of populations were probed by numerical simulations. Results revealed that spatial diffusion and fear both broaden the dynamical properties of this model, facilitating the emergence of periodic solutions and the formation of biodiversity.

Keywords: predator-prey model; reaction-diffusion; fear effect; Turing instability; Hopf bifurcation

1. Introduction

Recently, one of the hot issues in the ecosystem being studied is the impact of fear effect on the dynamics of prey and predators in predator-prey models. The fear effect is an inherent psychological reaction of the organisms to increase alertness and respond to danger [1]. It can trigger various anti-predation responses, such as changing the reproduction capacity and strategies [2], changing foraging behaviors and selecting new habitats [3], and reducing the birth and survival rate of offspring [4]. In 2020, Sarkara and Khajanchi [5] proposed the following predator-prey model that introduces the

cost of fear into the prey

$$\begin{cases} \dfrac{\mathrm{d}u}{\mathrm{d}t} = r_0 u\left(\eta + \dfrac{\alpha(1-\eta)}{\alpha+v}\right) - d_1 u - \beta u^2 - \dfrac{auv}{1+bu}, \\ \dfrac{\mathrm{d}v}{\mathrm{d}t} = \dfrac{\theta auv}{1+bu} - d_2 v, \end{cases} \tag{1.1}$$

where u and v, respectively, represent the densities of prey and predator. The meaning of the parameters can refer to [5]. In addition, in [5], $g(\eta, \alpha, v) = \eta + \frac{\alpha(1-\eta)}{\alpha+v}$ stands for a fear function which describes that the prey is affected by the fear of predator. So, we know some characteristics of $g(\eta, \alpha, v)$ showing $\lim_{\alpha\to\infty} g(\eta, \alpha, v) = 1$, $\lim_{v\to\infty} g(\eta, \alpha, v) = \eta$, $g(0, \alpha, v) = \frac{\alpha}{\alpha+v}$, $g(\eta, 0, v) = \eta$, $g(\eta, \alpha, 0) = 1$, $g(1, \alpha, v) = 1$, $\frac{\partial g}{\partial \eta} > 0$, $\frac{\partial g}{\partial \alpha} > 0$, $\frac{\partial g}{\partial v} < 0$, which imply that the inhibitory effect of fear on the birth rate of prey will increase with the increase of predator population and will decrease with the enhancement of the ability to identify the capture of predator.

In model (1.1), $\frac{au}{1+bu}$ stands for the Holling II functional response [6], which expresses the prey consumed by each predator per unit time, which only depends on the density of prey without being disturbed by the predator. It is of great significance to use different functional response functions to describe the relationship between prey and predator, which is caused by the difficulty of capturing the prey by the predator and the different absorption conversion rates of the predator. As we all know, the Beddington-DeAngelis (B-D) functional response function [7, 8] is described as $\frac{u}{1+au+bv}$, which depends on both the density of prey and predator populations. Assume that $b = 0$, the B-D functional response becomes the Holling II functional response, which implies that it is more comprehensive and accurate in describing the interference and handling of populations. In 1960, Leslie and Gower [9] proposed a novel functional response $\frac{v}{cu}$ to describe the conversion rate of prey to predator, called the Leslie-Gower (L-G) functional response. Compared with the Holling II functional response, the L-G functional response is affected by prey and interfered with by predators [10]. Therefore, the Holling II functional response function in model (1.1) can be replaced by the B-D functional response and L-G functional response, respectively, to study further the impact of different functional response functions on populations. Therefore, we consider the following predator-prey model, in which prey is subject to B-D functional response and predator is subject to modified L-G functional response

$$\begin{cases} \dfrac{\mathrm{d}u}{\mathrm{d}t} = r_0 u\left(\eta + \dfrac{\alpha(1-\eta)}{\alpha+v}\right) - d_0 u - \beta u^2 - \dfrac{(1-\delta)uv}{a_1 + (1-\delta)u + e(1-\delta)v}, \\ \dfrac{\mathrm{d}v}{\mathrm{d}t} = v\left(b - \dfrac{cv}{a_2 + (1-\delta)u}\right), \end{cases} \tag{1.2}$$

where the meaning of the parameters are the same as model (1.1), b is the growth rate of predator, and δ stands for the strength of prey refuge [11] with $\delta \in [0, 1)$. $\frac{u}{a_1+u+ev}$ represents the B-D functional response. $\frac{cv}{a_2+u}$ represents a modified L-G functional response, where c is the maximum value of the diminishment rate of predator due to prey, and a_2 measures the extent to which environment provides predator.

To explore how the fear effect acts on the populations, many scholars have constructed and studied a large number of models with different functional response functions. For example, Wang et al. [12] as well as Sarkara and Khajanchi [5], both proposed a predator-prey model with fear and Holling II. They all found that prey and predator populations were affected by fear effect. Pal et al. [13]

constructed a B-D predator-prey model with fear, which found that fear has a destructive effect on stability. Wang et al. [14] investigated an improved L-G predator-prey model with fear. They found that as the degree of fear increases, it will lead to a decrease in population density and the extinction of prey.

For simplicity, let $x = \frac{c}{a_1}u, y = \frac{c}{a_2 b}v, \tau = bt$, and model (1.1) can transform into the following simplified model (for simplicity, u, v, t represent x, y, τ again, respectively):

$$\begin{cases} \dfrac{\mathrm{d}u}{\mathrm{d}t} = u\left(\dfrac{\theta}{1+Kv} + r - \gamma u - \dfrac{v}{p+hu+mv}\right), \\ \dfrac{\mathrm{d}v}{\mathrm{d}t} = v\left(1 - \dfrac{v}{1+qu}\right), \end{cases} \tag{1.3}$$

where $r = \frac{r_0\eta - d_0}{b}$, $\gamma = \frac{a_1\beta}{bc}$, $\theta = \frac{r_0(1-\eta)}{b}$, $K = \frac{a_2 b}{c\alpha}$, $p = \frac{a_1 c}{a_2(1-\delta)}$, $q = \frac{a_1(1-\delta)}{a_2 c}$, $h = \frac{a_1}{a_2}$, $m = be$. Here, r can be positive or negative. Now, we give an analysis of the nature of r as follows:

(1) When $r_0\eta > d_0$, that is, $1 > \eta > \frac{d_0}{r_0}$, we have $r > 0$, which means that when the cost of minimum fear is high, the birth rate of prey affected by fear is higher than the mortality rate of prey.
(2) When $r_0\eta < d_0$, that is, $\frac{d_0}{r_0} > \eta > 0$, one has $r < 0$, which means that when the cost of minimum fear is small, the birth rate of prey affected by fear effect is lower than the mortality rate of prey.
(3) When $\eta = 1$, i.e., without the effect of the fear effect, we have $r_0 > d_0$, which means that the birth rate is higher than the mortality rate, which is consistent with the actual situation of biological species in the ecosystem.
(4) $\theta + r$ represents the natural growth rate of prey, which is greater than 0, meaning that prey will survive for a long time.

Then, some natural questions arise from model (1.3):

- What are the conditions for the existence and stability of the equilibria?
- What are the conditions for the occurrence of Hopf bifurcation, and, if so, how to determine its stability and direction?

On the other hand, species not only evolve on the timescale but also move randomly on the spatial scale. So, it is inevitable to consider the issues of species in time and space. In 1952, Turing [15] first described the movement of species on time and space scales via using the reaction-diffusion equations. He found that the steady state equilibrium in the spatial model is stable in the absence of diffusion but transforms unstable in the presence of diffusion, which means that diffusion can induce instability of populations [16, 17]. In addition to the instability driven by diffusion, the reaction-diffusion system also can be triggered by other mechanisms, such as steady states solutions [18], Hopf bifurcation [19], pattern formation and etc [20]. Han et al. [21] considered a modified L-G predator-prey model with cross-diffusion and indirect predation effect, which shows that cross-diffusion can drive Turing instability and pattern formation. Tiwari et al. [22] proposed and analyzed a B-D predator-prey interaction model with fear. They investigated some properties of bifurcation, such as Hopf bifurcation and pitchfork bifurcation.

Motivated by these works, we construct a reaction-diffusion predator-prey model as follows

$$\begin{cases} \dfrac{\partial u}{\partial t} = d_1\Delta u + u\left(\dfrac{\theta}{1+Kv} + r - \gamma u - \dfrac{v}{p+hu+mv}\right), \ x \in \Omega, t > 0, \\ \dfrac{\partial v}{\partial t} = d_2\Delta v + v\left(1 - \dfrac{v}{1+qu}\right), \ x \in \Omega, t > 0, \\ \dfrac{\partial u}{\partial \mathbf{n}} = \dfrac{\partial v}{\partial \mathbf{n}} = 0, \ x \in \partial\Omega, t > 0, \\ u(x,0) \geq 0, \ v(x,0) \geq 0, \ x \in \Omega, \end{cases} \tag{1.4}$$

where $d_1 \geq 0$ and $d_2 \geq 0$ are, respectively, the diffusion rate of prey and predator. Laplacian operator $\Delta = \frac{\partial^2}{\partial x^2}$ is in the one-dimensional diffusion, $\Delta = \frac{\partial^2}{\partial x^2} + \frac{\partial^2}{\partial y^2}$ is in the two-dimensional diffusion, $\Delta = \frac{\partial^2}{\partial x^2} + \frac{\partial^2}{\partial y^2} + \frac{\partial^2}{\partial z^2}$ is in the three-dimensional diffusion, $\Omega \subset \mathbb{R}^n$ is a bounded domain with smooth boundary $\partial\Omega$, and $\mathbf{n}$ is the outward unit normal vector of the boundary $\partial\Omega$ as in [23]. There is no population flux across the boundaries owing to homogeneous Neumann boundary conditions. Then, we ask:

- What are the critical conditions that determine Turing instability?
- What are the conditions for the occurrence of the spatially homogeneous and spatial inhomogeneous periodic solutions?
- If spatial homogeneous and spatial inhomogeneous periodic solutions occur, what are the conditions for determining the stability and direction?

The rest of the paper is organized as follows. In Section 2, we focus on discussing the existence and stability of the equilibria and give the Hopf bifurcation analysis of the nonspatial model (1.3). In Section 3, we investigate the Hopf bifurcation analysis of the spatial model (1.4). In Section 4, we present a series of numerical simulations to reveal the theoretical analysis.

2. Analysis of the nonspatial model (1.3)

2.1. Positivity and boundedness

From the nonspatial model (1.3), one has

$$\begin{aligned} u(t) =& u(0)\exp\left(\int_0^t \left[\frac{\theta}{1+Kv(s)} + r - \gamma u(s) - \frac{v(s)}{p+hu(s)+mv(s)}\right]\mathrm{d}s\right), \\ v(t) =& v(0)\exp\left(\int_0^t \left[1 - \frac{v(s)}{1+qu(s)}\right]\mathrm{d}s\right). \end{aligned}$$

We know $u(t), v(t) \geq 0$ based on the above two expressions. Then, $\mathbb{R}^2_+ = \{u > 0, v > 0\}$ is positively invariant for the nonspatial model (1.3).

Lemma 2.1. *All solutions $(u(t), v(t))$ of model (1.3) are contained in the region $U = \left\{(u,v) \in \mathbb{R}^2_+ : 0 \leq u(t) \leq \frac{r+\theta}{\gamma}, 0 \leq v(t) \leq 1 + \frac{q(r+\theta)}{\gamma}\right\}$ as $t \to +\infty$.*

2.2. Existence of equilibria

Define thresholds

$$R_0 = \theta + r,\ \theta^* = \frac{(1+K)[1-r(p+m)]}{p+m}.$$

From model (1.3), we denote

$$\begin{cases} H_1(u,v) = u\left(\dfrac{\theta}{1+Kv} + r - \gamma u - \dfrac{v}{p+hu+mv}\right), \\ H_2(u,v) = v\left(1 - \dfrac{v}{1+qu}\right). \end{cases} \tag{2.1}$$

Clearly, model (1.3) has three boundary equilibrium points: $E_0 = (0,0)$, $E_1 = \left(\frac{\theta+r}{\gamma}, 0\right)$, $E_2 = (0,1)$, where E_0 and E_2 always exist, and E_1 existes when $R_0 > 0$.
By solving (2.1), we obtain that $v = 1 + qu$ and

$$A_0u^3 + A_1u^2 + A_2u + A_3 = 0, \tag{2.2}$$

where

$$\begin{aligned} A_0 &= \gamma Kq(h+mq), \\ A_1 &= \gamma[(1+K)(h+mq) + Kq(p+m)] + Kq^2 - Krq(h+mq), \\ A_2 &= \gamma(1+K)(p+m) + q(1+2K) - r[(1+K)(h+mq) + Kq(p+m)] - \theta(h+mq), \\ A_3 &= (1+K)[1-r(p+m)] - \theta(p+m). \end{aligned}$$

It is obvious that Eq (2.2) is a third-order algebraic equation, which has one, two, or three positive roots. Hence, discussing the number of positive equilibria of model (1.3) is equivalent to discussing the number of positive roots of Eq (2.2).

First, let

$$\begin{aligned} f(u) &= A_0u^3 + A_1u^2 + A_2u + A_3, \\ \Delta_1 &= A_1^2 - 3A_0A_2, \\ \Delta_2 &= A_1^2A_2^2 - 27A_0^2A_3^2 - 4A_1^3A_3 - 4A_0A_2^3 + 18A_0A_1A_2A_3. \end{aligned}$$

From Eq (2.2), we know $A_0 > 0$, and the signs of A_1, A_2 and A_3 are uncertain. First, we discuss the sign of A_3.

(1) When $R_0 > 0$ and $r > 0$ hold, that is, $\theta + r > 0$ and $1 > \eta > \frac{d_0}{r_0}$, if $\frac{1}{p+m} > r$, we know that $1 - r(p+m) > 0$, which can be obtained that $A_3 > 0$ when $\theta < \theta^*$, $A_3 < 0$ when $\theta > \theta^*$, or $A_3 = 0$ when $\theta = \theta^*$; if $\frac{1}{p+m} \le r$, we know that $1 - r(p+m) \le 0$, which we can get that $A_3 < 0$.

(2) When $R_0 > 0$ holds, if $r < 0$, that is, $\frac{d_0}{r_0} > \eta > 0$, which implies that $1 - r(p+m) > 0$, then we get that $A_3 > 0$ when $\theta < \theta^*$, $A_3 < 0$ when $\theta > \theta^*$, or $A_3 = 0$ when $\theta = \theta^*$.

(3) When $R_0 > 0$ and $r = 0$ hold, we know that $A_3 > 0$ when $\frac{1+K}{p+m} > \theta > 0$, that is, $\theta < \theta^*$, $A_3 < 0$ when $\theta > \theta^*$, or $A_3 = 0$ when $\theta = \theta^*$.

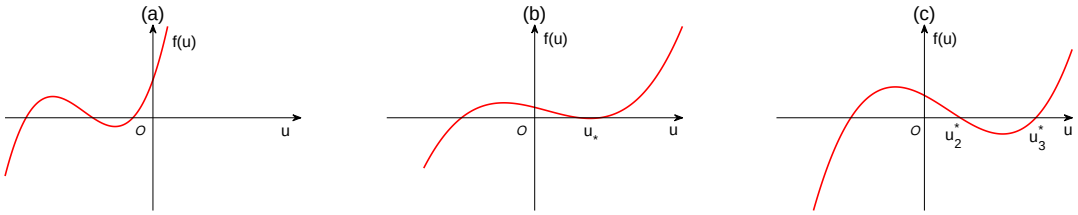

Figure 1. The positive roots of $f(u) = 0$ when $A_3 \geq 0$.

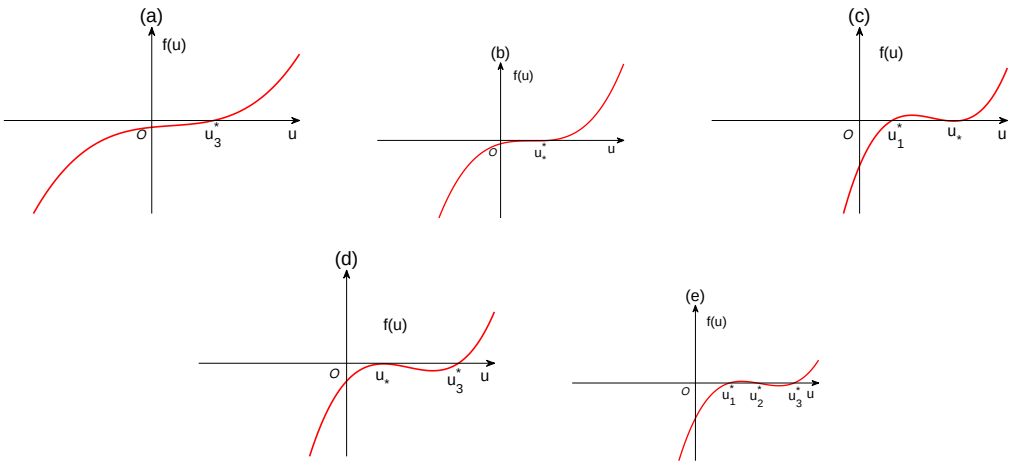

Figure 2. The positive roots of $f(u) = 0$ when $A_3 < 0$.

Therefore, we get the following lemma:

Lemma 2.2. *Regarding the sign of A_3, we have*

(1) $A_3 \geq 0$ *if* $(\mathbf{S_1})$: $R_0 > 0,\ \theta \leq \theta^*,\ \dfrac{1}{p+m} > r;$

(2) $A_3 < 0$ *if* $(\mathbf{S_2})$: $R_0 > 0,\ \theta > \theta^*,\ \dfrac{1}{p+m} > r;$

(3) $A_3 < 0$ *if* $(\mathbf{S_3})$: $R_0 > 0,\ r > 0,\ \dfrac{1}{p+m} \leq r.$

From Lemma 2.2(1), we know that $A_3 \geq 0$ when $(\mathbf{S_1})$ holds, which means that Eq (2.2) has at most two positive roots (see Figure 1). Next, by discussing the sign of Δ_2, we obtain the number of positive roots of Eq (2.2), seeing the following lemma:

Lemma 2.3. *Suppose that* $(\mathbf{S_1})$ *holds. Then, we have*

(1) *if $\Delta_2 < 0$, then Eq (2.2) has no positive root;*

(2) *if $\Delta_2 = 0$, then Eq (2.2) has a unique positive root;*

(3) *if $\Delta_2 > 0$, then Eq (2.2) has two different positive roots.*

From Lemma 2.2(2),(3), we know that $A_3 < 0$ when $(\mathbf{S_2})$ or $(\mathbf{S_3})$ holds, which means that Eq (2.2) has at least one positive root and at most three positive roots (see Figure 2). Then, by discussing the sign of Δ_1 and Δ_2, one has the following lemma:

Lemma 2.4. *Suppose that* $(\mathbf{S_2})$ *or* $(\mathbf{S_3})$ *holds. We obtain*

(1) *if* $\Delta_2 < 0$*, then Eq (2.2) has a unique positive root;*

(2) *if* $\Delta_2 = 0$*, and*

(i) $\Delta_1 = 0$*, then Eq (2.2) has a unique positive root;*
(ii) $\Delta_1 > 0$*, then Eq (2.2) has two positive roots;*

(3) *if* $\Delta_2 > 0$*, then Eq (2.2) has three different positive roots.*

Therefore, summarizing the above lemmas, we obtain the following theorem (for convenience, we summarize Theorem 2.1 in Table 1).

Table 1. The existence of the equilibria of model (1.3).

Condition			Equilibria
$R_0 < 0$			E_0, E_2
$R_0 > 0$	$\theta \le \theta^*$ $\frac{1}{p+m} > r$	$\Delta_2 > 0$	$E_0, E_1, E_2, E_2^*, E_3^*$
		$\Delta_2 = 0$	E_0, E_1, E_2, E_*
		$\Delta_2 < 0$	E_0, E_1, E_2
	$\theta > \theta^*$ $\frac{1}{p+m} > r$	$\Delta_2 > 0$	$E_0, E_1, E_2, E_1^*, E_2^*, E_3^*$
		$\Delta_2 = 0, \Delta_1 > 0$	$E_0, E_1, E_2, E_*, E_1^*(or\ E_3^*)$
		$\Delta_2 = 0, \Delta_1 = 0$	E_0, E_1, E_2, E_*^*
		$\Delta_2 < 0$	E_0, E_1, E_2, E_3^*
	$r > 0$ $\frac{1}{p+m} \le r$	$\Delta_2 > 0$	$E_0, E_1, E_2, E_1^*, E_2^*, E_3^*$
		$\Delta_2 = 0, \Delta_1 > 0$	$E_0, E_1, E_2, E_*, E_1^*(or\ E_3^*)$
		$\Delta_2 = 0, \Delta_1 = 0$	E_0, E_1, E_2, E_*^*
		$\Delta_2 < 0$	E_0, E_1, E_2, E_3^*

Theorem 2.1. **(I)** *Model (1.3) has a unique trivial equilibrium* $E_0 = (0, 0)$ *and one semi-trivial equilibrium* $E_2 = (0, 1)$*;*

(II) *if* $R_0 > 0$*, model (1.3) also has a semi-trivial equilibrium* $E_1 = (u_1, 0) = \left(\frac{\theta+r}{\gamma}, 0\right)$*;*

(III) *when* $(\mathbf{S_1})$ *holds, model (1.3) has at most two positive equilibria. Moreover,*

(1) if $\Delta_2 > 0$*, then model (1.3) has two different positive equilibria* $E_i^*(i = 2, 3)$*;*
(2) if $\Delta_2 = 0$*, then model (1.3) has a unique positive equilibrium* E_**;*
(3) if $\Delta_2 < 0$*, then model (1.3) has no positive equilibrium;*

(IV) *when* $(\mathbf{S_2})$ *or* $(\mathbf{S_3})$ *holds, model (1.3) has at least one positive equilibrium and at most three positive equilibria. Moreover,*

(1) if $\Delta_2 > 0$*, then model (1.3) has three different positive equilibria* $E_i^*(i = 1, 2, 3)$*;*

(2) if $\Delta_2 = 0$*, and*

(i) $\Delta_1 > 0$*, then model (1.3) has two positive equilibria* E_* *and* $E_1^*(or E_3^*)$*;*

(ii) $\Delta_1 = 0$*, then model (1.3) has a unique positive equilibrium* $E_*^* = \left(-\frac{A_1}{3A_0}, 1 - \frac{qA_1}{3A_0}\right)$*;*

(3) if $\Delta_2 < 0$*, then model (1.3) has a unique positive equilibrium* E_3^**.*

2.3. Stability of equilibria

For model (1.3), there is at least one positive equilibrium and at most three. Consequently, there are numerous rich and complex dynamical characteristics, which increases the difficulty in studying the dynamical properties of this model. Therefore, in order to alleviate the complexity of this study, we will only consider the case with a unique positive equilibrium, denoted as E^*. So in the subsequent research, we consistently assume that model (1.3) has a unique positive equilibrium, namely, $E^*(u^*, v^*)$.

Theorem 2.2. (I) *E_0 and E_1 are always hyperbolic saddle;*

(II) *(1) if* $R_0 > 0$*,* $\theta \le \theta^*$*,* $\frac{1}{p+m} > r$*, then E_2 is a stable node;*

(2) if one of the conditions hold

(i) $R_0 > 0$*,* $\theta > \theta^*$*,* $\frac{1}{p+m} > r$*;*

(ii) $R_0 > 0$*,* $\frac{1}{p+m} \le r$*,*

then E_2 is a hyperbolic saddle;

(3) if $R_0 > 0$*,* $\theta = \theta^*$*,* $\frac{1}{p+m} > r$*, then E_2 is a degenerate equilibrium.*

Proof. The corresponding Jacobian matrix for equilibria $E = (u, v)$ of model (1.3) is easily obtained as follows:

$$J_E = \begin{pmatrix} a_{11} & a_{12} \\ a_{21} & a_{22} \end{pmatrix},$$

where

$$\begin{aligned} a_{11} &= \frac{\theta}{1+Kv} + r - 2\gamma u - \frac{v}{p+hu+mv} + \frac{huv}{(p+hu+mv)^2}, \\ a_{12} &= -\left(\frac{\theta K u}{(1+Kv)^2} + \frac{u(p+hu)}{(p+hu+mv)^2}\right), \\ a_{21} &= \frac{qv^2}{(1+qu)^2},\ a_{22} = 1 - \frac{2v}{1+qu}. \end{aligned}$$

We can obtain the following characteristic equation:

$$\lambda^2 - \mathrm{tr}(J_E)\lambda + \det(J_E) = 0,$$

where

$$\mathrm{tr}(J_E) = a_{11} + a_{22},\ \det(J_E) = a_{11}a_{22} - a_{12}a_{21}.$$

(I) For equilibrium E_0 and E_1, it is obvious that one of the eigenvalues is $\lambda = 1 > 0$, then E_0 and E_1 are hyperbolic saddle.

(II) For equilibrium E_2, we obtain

$$\begin{aligned} \mathrm{tr}(J_{E_2}) &= \frac{\theta}{1+K} + r - \frac{1}{p+m} - 1, \\ \det(J_{E_2}) &= \frac{1}{p+m} - \frac{\theta}{1+K} - r. \end{aligned}$$

It is obvious that the sign of $\det(J_{E_2})$ is equivalent to the sign of A_3. Then, from Lemma 2.2, we know the sign of $\det(J_{E_2})$. Hence, when $R_0 > 0$, $\theta \le \theta^*$, $\frac{1}{p+m} > r$, we have $\mathrm{tr}(J_{E_2}) < 0$ and $\det(J_{E_2}) > 0$, which imply that E_2 is a stable node. When $(\mathbf{S_2})$ or $(\mathbf{S_3})$ holds, we have $\det(J_{E_2}) < 0$, which implies that E_2 is a hyperbolic saddle. When $R_0 > 0$, $\theta = \theta^*$, $\frac{1}{p+m} > r$, we have $\det(J_{E_2}) = 0$, which implies that E_2 is a degenerate equilibrium. □

Theorem 2.3. *Assume that E^* exists, and*

(1) *if $\chi > \max\{\chi^*, \chi^* + 1 - qb_{12}\}$, then E^* is stable;*

(2) *if $\chi < \min\{\chi^*, \chi^* + 1 - qb_{12}\}$, then E^* is unstable;*

(3) *if $\chi = \chi^*$ and $qb_{12} > 1$, then Hopf bifurcation occurs.*

Proof. For $E^*(u^*, v^*)$, we obtain

$$J_{E^*} = \begin{pmatrix} \chi^* - \chi + 1 & -b_{12} \\ q & -1 \end{pmatrix}, \tag{2.3}$$

where

$$\begin{aligned} \chi^* &= \frac{\theta}{1 + Kv^*} + r - 2\gamma u^* - 1, \\ \chi &= \frac{(p + mv^*)v^*}{(p + hu^* + mv^*)^2}, \\ b_{12} &= \frac{\theta K u^*}{(1 + Kv^*)^2} + \frac{u^*(p + hu^*)}{(p + hu^* + mv^*)^2}. \end{aligned}$$

Then we obtain the characteristic equation of E^*

$$\lambda^2 - \mathrm{tr}(J_{E^*})\lambda + \det(J_{E^*}) = 0,$$

where

$$\begin{aligned} \mathrm{tr}(J_{E^*}) &= \chi^* - \chi, \\ \det(J_{E^*}) &= -\chi^* + \chi - 1 + qb_{12}. \end{aligned}$$

By using the Routh-Hurwitz criterion, the conditions for the stability of E^* are established, that is to say, E^* is stable when $\chi > \max\{\chi^*, \chi^* + 1 - qb_{12}\}$, while E^* is unstable when $\chi < \min\{\chi^*, \chi^* + 1 - qb_{12}\}$.

When $\chi = \chi^*$ and $qb_{12} > 1$, we have $\mathrm{tr}(J_{E^*}) = 0$ and $\det(J_{E^*}) > 0$. Then, we have roots $\lambda_{1,2} = \pm i\sqrt{\det(J_{E^*})}$ at $\chi = \chi^*$. Choosing χ as a bifurcation parameter (in fact, θ is the control parameter), we have

$$\left[\frac{d(\mathrm{Re}\lambda(\chi))}{\mathrm{d}\chi}\right]\Big|_{\lambda = i\sqrt{\det(J_{E^*})}, \chi = \chi^*} = \frac{1}{2}\frac{\mathrm{d}(\mathrm{tr}(J_{E^*}))}{\mathrm{d}\chi}\Big|_{\chi = \chi^*} = -\frac{1}{2} \neq 0.$$

Hence, model (1.3) undergoes a Hopf bifurcation at $\chi = \chi^*$. □

Remark 2.1. *For positive equilibrium E^*, assume that $qb_{12} > 1$, and*

(1) *if $\chi > \chi^*$, then E^* is stable;*

(2) *if $\chi < \chi^*$, then E^* is unstable;*

(3) *if $\chi = \chi^*$, then E^* emerges Hopf bifurcation.*

That means that χ^* can determine the stability of E^*.

Remark 2.2. *(1) When $m = 0$ and $p = 0$, the B-D functional response of model (1.3) changes to linear approximations. In this case, the model has a unique positive equilibrium and exhibits limit cycles under fear interference.*

(2) When $m = 0$, the B-D functional response of model (1.3) becomes the Holling II functional response. In this case, the model still has a unique positive equilibrium and exhibits limit cycles under fear interference, but shows complexity compared to case (1). Readers can refer to the research results in [14].

Theorem 2.4. *Suppose that $R_0 > 0$, $\gamma > \frac{h}{pm}$, and $\sqrt{\frac{4}{1+q}\left(\gamma - \frac{h}{pm}\right)} > \left(\frac{1}{p} + q + \frac{rq^2}{\gamma}\right)$ hold. If*

$$\frac{\gamma}{K\gamma + q^2}\left[\sqrt{\frac{4}{1+q}\left(\gamma - \frac{h}{pm}\right)} - \left(\frac{1}{p} + q + \frac{rq^2}{\gamma}\right)\right] > \theta,$$

then E^* is globally asymptotically stable.

Proof. Denote

$$V(u, v) = u - u^* - u^* \ln \frac{u}{u^*} + v - v^* - v^* \ln \frac{v}{v^*}.$$

Then, we obtain

$$\begin{aligned}
\frac{\mathrm{d}V}{\mathrm{d}t} =& -\gamma(u-u^*)^2 + \frac{hv^*(u-u^*)^2 + (p+hu^*)(u-u^*)(v-v^*)}{(p+hu^*+mv^*)(p+hu+mv)} \\
&- \frac{K\theta(u-u^*)(v-v^*)}{(1+Kv^*)(1+Kv)} + \frac{qv^*(u-u^*)(v-v^*) - (1+qu^*)(v-v^*)^2}{(1+qu^*)(1+qu)} \\
\leq& -\left(\gamma - \frac{h}{pm}\right)|u-u^*|^2 - \frac{1}{1+q}|v-v^*|^2 + \left(K\theta + \frac{1}{p} + q + \frac{q^2(\theta+r)}{\gamma}\right)|u-u^*||v-v^*| \\
=& -B_1(|u-u^*|^2 - \frac{B_3}{2B_1}|u-u^*||v-v^*|) - B_2|v-v^*|^2 \\
=& -B_1\left(|u-u^*|^2 - \frac{B_3}{2B_1}|u-u^*||v-v^*| - \frac{B_3^2}{4B_1^2}|v-v^*|^2\right) - \left(B_2 - \frac{B_3^2}{4B_1}\right)|v-v^*|^2 \\
=& -B_1\left(|u-u^*| - \frac{B_3}{2B_1}|v-v^*|\right)^2 - \left(B_2 - \frac{B_3^2}{4B_1}\right)|v-v^*|^2,
\end{aligned}$$

where $B_1 = \gamma - \frac{h}{pm}$, $B_2 = \frac{1}{1+q}$, $B_3 = K\theta + \frac{1}{p} + q + \frac{q^2(\theta+r)}{\gamma}$.

Since conditions $R_0 > 0$, $\gamma > \frac{h}{pm}$, and $\sqrt{\frac{4}{1+q}\left(\gamma - \frac{h}{pm}\right)} > \left(\frac{1}{p} + q + \frac{rq^2}{\gamma}\right)$ hold, we obtain $B_2 > \frac{B_3^2}{4B_1}$ when

$$\left(\gamma - \frac{h}{pm}\right) > \frac{1+q}{4}\left(K\theta + \frac{1}{p} + q + \frac{q^2(\theta+r)}{\gamma}\right)^2,$$

which imply that $\frac{\mathrm{d}V}{\mathrm{d}t} < 0$. Then, the proof is finished. □

2.4. Hopf bifurcation

Theorem 2.5. *Assume that $R_0 > 1$, $qb_{12} > 1$, and $\chi = \chi^*$ hold, periodic solutions bifurcated from Hopf bifurcation are stable (unstable) and the direction is subcritical (supercritical) when $\Upsilon(\chi^*) < 0 (> 0)$.*

Proof. Let $U = u - u^*$ and $V = v - v^*$, and we can transform model (1.3) (for brevity, u and v stand for U and V, respectively) to

$$\begin{cases} \dfrac{\mathrm{d}u}{\mathrm{d}t} =(u+u^*)\left(\dfrac{\theta}{1+K(v+v^*)} + r - \gamma(u+u^*) - \dfrac{v+v^*}{p+h(u+u^*)+m(v+v^*)}\right), \\ \dfrac{\mathrm{d}v}{\mathrm{d}t} =(v+v^*)\left(1 - \dfrac{v+v^*}{1+q(u+u^*)}\right). \end{cases} \tag{2.4}$$

Rewrite model (2.4) as

$$\begin{pmatrix} u_t \\ v_t \end{pmatrix} = J_{E^*}\begin{pmatrix} u \\ v \end{pmatrix} + \begin{pmatrix} g(u,v,\chi) \\ h(u,v,\chi) \end{pmatrix}, \tag{2.5}$$

where J_{E^*} is denoted in (2.3) and

$$\begin{cases} g(u,v,\chi) =g_{20}u^2 + g_{11}uv + g_{02}v^2 + g_{30}u^3 + g_{21}u^2v + g_{12}uv^2 + g_{03}v^3 + O(|(u,v)|^4), \\ h(u,v,\chi) =h_{20}u^2 + h_{11}uv + h_{02}v^2 + h_{30}u^3 + h_{21}u^2v + h_{12}uv^2 + h_{03}v^3 + O(|(u,v)|^4), \end{cases}$$

with

$$g_{20} = -\gamma + \frac{h\chi}{p+hu+mv},\ g_{11} = -\left(\frac{\theta K}{(1+Kv^*)^2} + \frac{p^2+hpu^*+mpv^*+2hmu^*v^*}{(p+hu^*+mv^*)^3}\right),$$

$$g_{02} = \frac{\theta K^2u^*}{(1+Kv^*)^3} + \frac{mu^*(p+hu^*)}{(p+hu^*+mv^*)^3},\ g_{21} = \frac{h(p^2+hpu^*-m^2v^{*2}+2hmu^*v^*)}{(p+hu^*+mv^*)^3},$$

$$g_{12} = \frac{\theta K^2}{(1+Kv^*)^3} + \frac{m(p^2-h^2u^{*2}+mpv^*+2hmu^*v^*)}{(p+hu^*+mv^*)^4},\ g_{30} = -\frac{h^2\chi}{(p+hu^*+mv^*)^2},$$

$$g_{03} = \frac{\theta K^3u^*}{(1+Kv^*)^4} + \frac{m^2u^*(p+hu^*)}{(p+hu^*+mv^*)^4},\ h_{20} = -\frac{q^2}{1+qu^*},\ h_{11} = \frac{q}{1+qu^*},$$

$$h_{02} = -\frac{1}{1+qu^*},\ h_{30} = \frac{q^3}{(1+qu^*)^2},\ h_{21} = -\frac{q^2}{(1+qu^*)^2},\ h_{12} = \frac{2q}{(1+qu^*)^2},\ h_{03} = 0.$$

Assuming that J_{E^*} has two characteristic roots, it can be written as $\lambda_{1,2}(\chi) = \varphi(\chi) \pm i\psi(\chi)$, where

$$\varphi(\chi) = \frac{\chi^* - \chi}{2},\ \psi(\chi) = \sqrt{-\chi^* + \chi - 1 + qb_{12} - \varphi^2}.$$

Obviously, eigenvalues $\lambda_1(\chi)$ and $\lambda_2(\chi)$ are complex conjugate if $-\chi^* + \chi - 1 + qb_{12} > \varphi^2$. Then, the eigenvectors of J_{E^*} corresponding to the eigenvalues of $\lambda(\chi) = i\psi(\chi)$ at $\chi = \chi^*$ are given by

$$\xi = \begin{bmatrix} 1 \\ \xi_1 - i\xi_2 \end{bmatrix},$$

where $\xi_1 = \frac{\chi^*-\chi+2}{2b_{12}}$, $\xi_2 = \frac{\psi(\chi)}{b_{12}}$.

Based on the transformation $(u,v)^T = \begin{pmatrix} 1 & 0 \\ \xi_1 & \xi_2 \end{pmatrix}(x,y)^T$, model (2.5) becomes

$$\begin{bmatrix} \frac{\mathrm{d}x}{\mathrm{d}t} \\ \frac{\mathrm{d}y}{\mathrm{d}t} \end{bmatrix} = \begin{bmatrix} \varphi(\chi) & -\psi(\chi) \\ \psi(\chi) & \varphi(\chi) \end{bmatrix}\begin{bmatrix} x \\ y \end{bmatrix} + \begin{bmatrix} \Phi(x,y) \\ \Psi(x,y) \end{bmatrix}, \tag{2.6}$$

where

$$\begin{aligned}\Phi(x,y) =&[g_{20}+g_{11}\xi_1+g_{02}\xi_1^2]x^2+[g_{11}+2g_{02}\xi_1]\xi_2xy+g_{02}\xi_2^2y^2\\&+[g_{30}+g_{21}\xi_1+g_{12}\xi_1^2+g_{03}\xi_1^3]x^3+[g_{12}+3g_{03}\xi_1]\xi_2^2xy^2,\\\Psi(x,y) =&\frac{1}{\xi_2}[h_{20}+(h_{11}-g_{20})\xi_1+(h_{02}-g_{11})\xi_1^2-g_{02}\xi_1^3]x^2\\&+[h_{11}+(2h_{02}-g_{11})\xi_1-2g_{02}\xi_1^2]xy+(h_{02}-g_{02}\xi_1)\xi_2y^2\\&-g_{03}\xi_1\xi_2^2y^3+[h_{21}+(2h_{12}-g_{21})\xi_1-2g_{12}\xi_1^2-3g_{03}\xi_1^3]x^2y.\end{aligned}$$

Next, we calculate the 1st Lyapunov coefficient as follows:

$$\begin{aligned}\Upsilon(\chi^*) =&\frac{1}{16}[\Phi_{xxx}+\Phi_{xyy}+\Psi_{xxy}+\Psi_{yyy}]_{(0,0,\chi^*)}\\&+\frac{1}{16\psi(\chi^*)}[\Phi_{xy}(\Phi_{xx}+\Phi_{yy})-\Psi_{xy}(\Psi_{xx}+\Psi_{yy})-\Phi_{xx}\Psi_{xx}+\Phi_{yy}\Psi_{yy}]_{(0,0,\chi^*)},\end{aligned}$$

where

$$\begin{aligned}&\Phi_{xxx}(0,0,\chi^*)=6(g_{30}+g_{21}\xi_1+g_{12}\xi_1^2+g_{03}\xi_1^3),\ \Phi_{xyy}(0,0,\chi^*)=2(g_{12}+3g_{03}\xi_1)\xi_2^2,\\&\Psi_{xxy}(0,0,\chi^*)=2[h_{21}+(2h_{12}-g_{21})\xi_1-6g_{12}\xi_1^2-3g_{03}\xi_1^3],\\&\Psi_{yyy}(0,0,\chi^*)=-6g_{03}\xi_1\xi_2^2,\ \Phi_{xx}(0,0,\chi^*)=2(g_{20}+g_{11}\xi_1+g_{02}\xi_1^2),\\&\Phi_{xy}(0,0,\chi^*)=(g_{11}+2g_{02}\xi_1)\xi_2,\ \Phi_{yy}(0,0,\chi^*)=2g_{02}\xi_2^2,\\&\Psi_{xx}(0,0,\chi^*)=\frac{2}{\xi_2}[h_{20}+(h_{11}-g_{20})\xi_1+(h_{02}-g_{11})\xi_1^2-g_{02}\xi_1^3],\\&\Psi_{xy}(0,0,\chi^*)=h_{11}+(2h_{02}-g_{11})\xi_1-2g_{02}\xi_1^2,\ \Psi_{yy}(0,0,\chi^*)=2(h_{02}-g_{02}\xi_1)\xi_2,\end{aligned}$$

owing to

$$\left[\frac{\partial(\mathrm{Re}\varphi(\chi))}{\partial\chi}\right]_{\chi=\chi^*}=-\frac{1}{2}<0.$$

Therefore, one gets the 1st Lyapunov coefficient $\Lambda=-\frac{\Upsilon(\chi^*)}{\varphi'(\chi^*)}$, which determines the stability and direction of Hopf bifurcating periodic solution. □

3. Analysis of the spatial model (1.4)

3.1. Stability of E^*

Let $0=\mu_0<\mu_1<\mu_2<\cdots<\mu_i<\cdots$ be the eigenvalues for the operator $-\Delta$ subject to the homogeneous Neumann boundary condition on Ω, where μ_i has multiplicity $m_i\geq 1$ and μ_1 is the smallest eigenvalue. Denote the real-valued Sobolev space $\mathbf{S}=\left\{(u,v)\in H^2(0,l\pi)\times H^2(0,l\pi):\frac{\partial u}{\partial\mathbf{n}}|_{\partial\Omega}=\frac{\partial v}{\partial\mathbf{n}}|_{\partial\Omega}=0\right\}$, and let $\mathbf{S}_{\mathbb{C}}=\mathbf{S}\oplus\mathbf{S}\mathrm{i}=\{s_1+s_2\mathrm{i}:s_1,s_2\in\mathbf{S}\}$. Denote $\mathbb{N}_0=\mathbb{N}\cup\{0\}$.

The linearization equation of model (1.4) at E^* is

$$\begin{pmatrix}\frac{\partial u}{\partial t}\\\frac{\partial v}{\partial t}\end{pmatrix}=D\begin{pmatrix}\Delta u\\\Delta v\end{pmatrix}+J_{E^*}\begin{pmatrix}u\\v\end{pmatrix},\tag{3.1}$$

where $D = \text{diag}(d_1, d_2)$ and J_{E^*} is denoted in (2.3).
Then, the characteristic equation of (3.1) is given by

$$\lambda^2 - \mathbf{Tr}(k)\lambda + \mathbf{Det}(k) = 0, \tag{3.2}$$

where

$$\mathbf{Tr}(k) = -(d_1 + d_2)k^2 + \chi^* - \chi,$$
$$\mathbf{Det}(k) = d_1 d_2 k^4 + [d_1 - (\chi^* - \chi + 1)d_2]k^2 - \chi^* + \chi - 1 + qb_{12}.$$

When condition $\chi > \max\{\chi^*, \chi^* + 1 - qb_{12}\}$ holds, then we have $\mathbf{Tr}(0) < 0$ and $\mathbf{Det}(0) > 0$, which imply that $\mathbf{Tr}(k) < 0$ always holds.

Next, we analyze the sign of $\mathbf{Det}(k)$. (1) if $\frac{d_1}{d_2} \geq \max\{0, \chi^* - \chi + 1\}$, we can obtain $\mathbf{Det}(k) > 0$;

(2) if $\frac{d_1}{d_2} < \chi^* - \chi + 1$, we need to discuss the sign of $\Delta = (d_1 - (\chi^* - \chi + 1)d_2)^2 + 4d_1 d_2(\chi^* - \chi + 1 - qb_{12})$,

(i) if $\Delta < 0$, which implies that $\mathbf{Det}(k) > 0$;

(ii) if $\Delta > 0$, which implies that $\mathbf{Det}(k)$ must have negative roots, then by calculating, we have $\mathbf{Det}(k) > 0$ when $-(\chi^* - \chi + 1) + 2qb_{12} - 2\sqrt{-qb_{12}(\chi^* - \chi + 1 - qb_{12})} < \frac{d_1}{d_2} < \chi^* - \chi + 1$, and $\mathbf{Det}(k) < 0$ when $-(\chi^* - \chi + 1) + 2qb_{12} - 2\sqrt{-qb_{12}(\chi^* - \chi + 1 - qb_{12})} > \frac{d_1}{d_2} > 0$.
Hence, the Theorem 3.1 is shown by the properties of E^* in model (1.4).

Theorem 3.1. *When $\chi > \max\{\chi^*, \chi^* + 1 - qb_{12}\}$ hold, and*

(1) *if*

$$\frac{d_1}{d_2} \geq \max\{0, \chi^* - \chi + 1\},$$

or

$$-(\chi^* - \chi + 1) + 2qb_{12} - 2\sqrt{-qb_{12}(\chi^* - \chi + 1 - qb_{12})} < \frac{d_1}{d_2} < \chi^* - \chi + 1,$$

then E^* is locally asymptotically stable;

(2) *if*

$$0 < \frac{d_1}{d_2} < -(\chi^* - \chi + 1) + 2qb_{12} - 2\sqrt{-qb_{12}(\chi^* - \chi + 1 - qb_{12})},$$

then E^* is unstable, and the Turing instability occurs.

Remark 3.1. *In Figure 3, the blue line represents the equation*

$$d_2 = \frac{1}{(\chi^* - \chi + 1) + 2qb_{12} - 2\sqrt{-qb_{12}(\chi^* - \chi + 1 - qb_{12})}} d_1,$$

and we can see that the red region is the region where Turing instability occurs, and the green region is the region where the steady state solution E^* is stable. On the other hand, it also shows that when the diffusion of predator is fixed, if the diffusion of prey is smaller, it is more difficult to maintain the stability of populations.

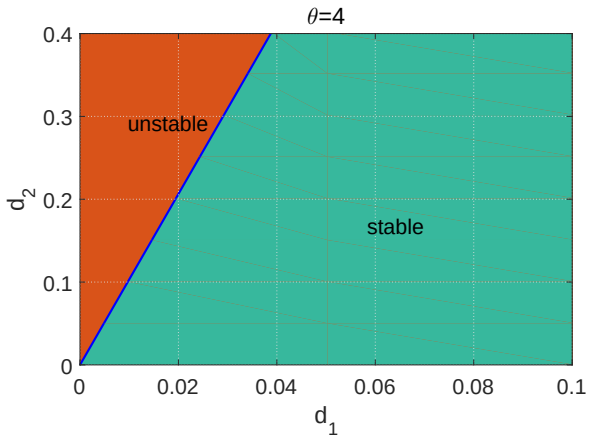

Figure 3. Diagram for Turing instability on $d_1 - d_2$ in model (1.4) with $\theta = 4$.

Theorem 3.2. *When $R_0 > 0$ and $\gamma > \frac{h}{pm}$ hold, if*

$$\frac{1}{2}\left(K\theta + \frac{1}{p} + q + \frac{q^2(\theta + r)}{\gamma}\right) < \min\left\{\frac{1}{1+q}, \gamma - \frac{h}{pm}\right\},$$

then E^* is globally asymptotically stable.

Proof. Denote a Lyapunov function

$$V = \int_\Omega \left(\int_{u^*}^{u} \frac{\xi - u^*}{\xi} \mathrm{d}\xi + \int_{v^*}^{v} \frac{\zeta - v^*}{\zeta} \mathrm{d}\zeta\right) \mathrm{d}x.$$

Then

$$\begin{aligned}
\frac{\mathrm{d}V}{\mathrm{d}t} =& \int_\Omega \left[\left(\frac{\theta}{1+Kv} + r - \gamma u - \frac{v}{p + hu + mv}\right)(u - u^*)\right] \mathrm{d}x \\
&+ \int_\Omega \left[\left(1 - \frac{v}{1+qu}\right)(v - v^*)\right] \mathrm{d}x - d_1 u^* \int_\Omega \frac{|\nabla u|^2}{u^2} \mathrm{d}x - d_2 v^* \int_\Omega \frac{|\nabla v|^2}{v^2} \mathrm{d}x \\
\leq& - \int_\Omega \left[\gamma - \frac{h}{pm} - \frac{1}{2}\left(K\theta + \frac{1}{p} + q + \frac{q^2(\theta + r)}{\gamma}\right)\right](u - u^*)^2 \mathrm{d}x - d_1 u^* \int_\Omega \frac{|\nabla u|^2}{u^2} \mathrm{d}x \\
&- \int_\Omega \left[\frac{1}{1+q} - \frac{1}{2}\left(K\theta + \frac{1}{p} + q + \frac{q^2(\theta + r)}{\gamma}\right)\right](v - v^*)^2 \mathrm{d}x - d_2 v^* \int_\Omega \frac{|\nabla v|^2}{v^2} \mathrm{d}x,
\end{aligned}$$

which is used in the inequality $a^2 + b^2 \geq 2ab$.

Then, under the Neumann boundary conditions and $\frac{1}{1+q} > \frac{1}{2}\left(K\theta + \frac{1}{p} + q + \frac{q^2(\theta+r)}{\gamma}\right)$, $\gamma > \frac{h}{pm} + \frac{1}{2}\left(K\theta + \frac{1}{p} + q + \frac{q^2(\theta+r)}{\gamma}\right)$, we obtain that $\frac{\mathrm{d}V}{\mathrm{d}t} \leq 0$, which implies that the proof of Theorem 3.2 is completed. □

3.2. Hopf bifurcation

3.2.1. Existence

Let $X = u - u^*$ and $Y = v - v^*$, and we can transform model (1.4) (for brevity, u and v represent X and Y again, respectively) to:

$$\begin{cases} \dfrac{\partial u}{\partial t} = d_1\Delta u + (u+u^*)\Big(\dfrac{\theta}{1+K(v+v^*)} + r - \gamma(u+u^*) - \dfrac{v+v^*}{p+h(u+u^*)+m(v+v^*)}\Big), \\ \dfrac{\partial v}{\partial t} = d_2\Delta v + (v+v^*)\left(1 - \dfrac{v+v^*}{1+q(u+u^*)}\right). \end{cases} \tag{3.3}$$

Then, model (3.3) can be rewritten as

$$\begin{cases} \dfrac{\partial u}{\partial t} = d_1\Delta u + g(u,v,\chi), \\ \dfrac{\partial v}{\partial t} = d_2\Delta v + h(u,v,\chi). \end{cases}$$

The linearized operator of model (3.3) at $(0,0,\chi)$ is given by

$$P(\chi) = \begin{pmatrix} d_1\Delta + b_{11}(\chi) & -b_{12}(\chi) \\ q & d_2\Delta - 1 \end{pmatrix},$$

where the domain of $P(\chi)$ is $\mathbb{S}_{\mathbb{C}}$ and

$$b_{11}(\chi) = \chi^* - \chi + 1,\ b_{12}(\chi) = \frac{\theta K u^*}{(1+Kv^*)^2} + \frac{u^*(p+hu^*)\chi}{v^*(p+mv^*)}.$$

Let $k = \frac{n^2}{l^2}$, where $\frac{n^2}{l^2}$ is the eigenvalue of $-u_{xx} \to u$ and its corrsponding eigenfunction is $\phi_n(x) = \cos\frac{n}{l}x$. Then, (3.2) becomes

$$\Lambda^2 - \mathbf{T}_n(\chi)\Lambda + \mathbf{D}_n(\chi) = 0,\ n = 0,1,2,\cdots,$$

where

$$\begin{aligned} \mathbf{T}_n(\chi) &= -(d_1+d_2)\frac{n^2}{l^2} + \chi^* - \chi, \\ \mathbf{D}_n(\chi) &= d_1d_2\frac{n^4}{l^4} + [d_1 - (\chi^* - \chi + 1)d_2]\frac{n^2}{l^2} - \chi^* + \chi - 1 + qb_{12}(\chi), \end{aligned} \tag{3.4}$$

and we obtain the eigenvalues

$$\Lambda(\chi) = \frac{\mathbf{T}_n(\chi) \pm \sqrt{\mathbf{T}_n^2(\chi) - 4\mathbf{D}_n(\chi)}}{2},\ n = 0,1,2,\cdots.$$

Let χ_0 be the possible Hopf bifurcation point satisfying conditions ($\mathbf{H_1}$): there exists $n \in \mathbb{N}_0$ such that

$$\mathbf{T}_n(\chi_0) = 0,\ \mathbf{D}_n(\chi_0) > 0,\ \mathbf{T}_j(\chi_0) \neq 0,\ \mathbf{D}_j(\chi_0) \neq 0\ for\ j \neq n, \tag{3.5}$$

and for the unique pair of complex eigenvalues $\rho(\chi) \pm \omega(\chi)$i near the imaginary axis

$$\rho'(\chi_0) \neq 0, \tag{3.6}$$

where

$$\rho(\chi) = -(d_1 + d_2)\frac{n^2}{2l^2} + \frac{\chi^* - \chi}{2},\ \omega(\chi) = \sqrt{\mathbf{D}_n(\chi) - \rho^2(\chi)}.$$

From (3.4), when $\chi > \max\{\chi^*, \chi^* + 1 + qb_{12}\}$, it is obvious that $\mathbf{T}_n(\chi_0) < 0$ and $\mathbf{D}_n(\chi_0) > 0$, which imply that (u^*, v^*) is stable. Thus, any potential bifurcation points shall be in $\chi < \min\{\chi^*, \chi^* + 1 - qb_{12}\}$. By calculating, we get

$$\rho'(\chi) = -\frac{1}{2}, \tag{3.7}$$

so the transversality condition (3.6) is always held.

(**1**) When $n = 0$, let $\chi_0^H = \chi^*$, then we find that χ_0^H is always a Hopf bifurcation point for $l > 0$ due to $\mathbf{T}_0(\chi_0^H) = 0$, $\mathbf{T}_j(\chi_0^H) < 0$ for any $j \geq 1$, and $\mathbf{D}_k(\chi_0^H) > 0$ for any $k \in \mathbb{N}$.

(**2**) When $n \geq 1$, since $b_{11}(\chi_0^H) = 0$, $b'_{11}(\chi) < 0$ for $\chi_0 < \chi^*$, we have $0 < b_{11}(\chi) < b_{11}(0) := \chi^* + 1$ for $\chi_0 < \chi^*$.

Denote

$$l_n = n\sqrt{\frac{d_1 + d_2}{\chi^* + 1}},\ n \in \mathbb{N}.$$

Then for $l_n < l < l_{n+1}$, and $1 \leq j \leq n$, let χ_j^H be the root of $\chi^* - \chi = (d_1 + d_2)\frac{n^2}{l^2}$, then it satisfies $\chi_0^H > \chi_j^H > 0$. Moreover, by $b'_{11}(\chi) < 0$ for $\chi_0 < \chi^*$, we obtain

$$0 < \chi_n^H < \cdots < \chi_3^H < \chi_2^H < \chi_1^H < \chi_0^H < \chi^*$$

and

$$\mathbf{T}_j(\chi_j^H) = 0,\ \mathbf{T}_i(\chi_j^H) \neq 0\ for\ i \neq j,\ 1 \leq j \leq n.$$

Now, it is demonstrated that $\mathbf{D}_n(\chi_j^H) > 0$ for $j \neq n$. For $\chi \in (0, \chi_0^H]$, we get

$$\mathbf{D}_n(\chi) = d_1 d_2 \frac{n^4}{l^4} + [d_1 - (\chi^* - \chi + 1)d_2]\frac{n^2}{l^2} - \chi^* + \chi - 1 + qb_{12}(\chi).$$

Obviously, $\mathbf{D}_n(\chi) = 0$ is a quadratic function of variable $\frac{n^2}{l^2}$, so we have $\mathbf{D}_n(\chi_j^H) > 0$ when

$$\frac{d_1}{d_2} \geq \max\{0, \chi^* - \chi + 1\},$$

or

$$-(\chi^* - \chi + 1) + 2qb_{12} - 2\sqrt{-qb_{12}(\chi^* - \chi + 1 - qb_{12})} < \frac{d_1}{d_2} < \chi^* - \chi + 1.$$

Theorem 3.3. *Assume that* $-(\chi^* - \chi + 1) + 2qb_{12} - 2\sqrt{-qb_{12}(\chi^* - \chi + 1 - qb_{12})} < \frac{d_1}{d_2} < \chi^* - \chi + 1$ *or* $\frac{d_1}{d_2} \geq \max\{0, \chi^* - \chi + 1\}$ *hold, and for any* $l \in (l_n, l_{n+1}]$, *there are n points* $\chi_j^H(l)$, $j \in [1, n]$ *satisfying*

$$0 < \chi_n^H < \cdots < \chi_3^H < \chi_2^H < \chi_1^H < \chi_0^H < \chi^*$$

such that Hopf bifurcation arises at each $\chi = \chi_j^H$.

3.2.2. Direction and stability

We apply the normal form theory and center manifold theorem [24, 25] to prove Theorems 3.4 and 3.5.

Theorem 3.4. *Assume the condition of Theorem 3.3 is satisfied, the bifurcating periodic solutions of spatial homogeneous are stable (unstable), and the direction is subcritical (supercritical) when* $\mathrm{Re}(c_1(\chi_0^H)) < 0 (> 0)$.

Proof. Let

$$\mathfrak{q} = (\mathfrak{a}_0, \mathfrak{b}_0)^T = \left(\frac{1+\omega_0 \mathrm{i}}{q}, 1\right)^T, \ \mathfrak{q}^* = (\mathfrak{a}_0^*, \mathfrak{b}_0^*)^T = \left(\frac{q}{2l\pi\omega_0}\mathrm{i}, \frac{\omega_0 - \mathrm{i}}{2l\pi\omega_0}\right)^T,$$

where $\omega_0 = \sqrt{-1 + qb_{12}(\chi_0^H)}$, such that $P(\chi_0)\mathfrak{q} = \omega_0 \mathfrak{q}\mathrm{i}$, $P^*(\chi_0^H)\mathfrak{q}^* = -\omega \mathfrak{q}^*\mathrm{i}$, $\langle \mathfrak{q}^*, \mathfrak{q}\rangle = 1$, and $\langle \mathfrak{q}^*, \overline{\mathfrak{q}}\rangle = 0$, where $\langle \mathfrak{p}, \mathfrak{q}\rangle = \int_0^{l\pi} \overline{\mathfrak{p}}^T \mathfrak{q} \mathrm{d}x$.

According to [25], we obtain that

$$\mathcal{E}_{\mathfrak{q}\mathfrak{q}} = (\mathfrak{c}_0, \mathfrak{d}_0)^T, \ \mathcal{E}_{\mathfrak{q}\overline{\mathfrak{q}}} = (\mathfrak{e}_0, \mathfrak{f}_0)^T, \ \mathcal{J}_{\mathfrak{q}\mathfrak{q}\overline{\mathfrak{q}}} = (\mathfrak{g}_0, \mathfrak{h}_0)^T,$$

where

$$\begin{aligned}
\mathfrak{c}_0 =& \frac{g_{uu}(1-\omega_0^2)}{q^2} + \frac{2g_{uv}}{q} + g_{vv} + \frac{2(g_{uu}+g_{uv})\omega_0 \mathrm{i}}{q},\\
\mathfrak{d}_0 =& \frac{h_{uu}(1-\omega_0^2)}{q^2} + \frac{2h_{uv}}{q} + h_{vv} + \frac{2(h_{uu}+h_{uv})\omega_0 \mathrm{i}}{q},\\
\mathfrak{e}_0 =& \frac{g_{uu}(1-\omega_0^2)}{q^2} + \frac{2g_{uv}}{q} + g_{vv}, \quad \mathfrak{f}_0 = \frac{h_{uu}(1-\omega_0^2)}{q^2} + \frac{2h_{uv}}{q} + h_{vv},\\
\mathfrak{g}_0 =& \frac{g_{uuu}(1-\omega_0^2)}{q^3} + \frac{3g_{uuv}(1-\omega_0^2)}{q^2} + \frac{3g_{uvv}}{q} + g_{vvv} + \left[\frac{g_{uuu}(1-\omega_0^2)}{q^3} + \frac{2g_{uuv}}{q^2} + \frac{g_{uvv}}{q}\right]\omega_0 \mathrm{i},\\
\mathfrak{h}_0 =& \frac{h_{uuu}(1-\omega_0^2)}{q^3} + \frac{3h_{uuv}(1-\omega_0^2)}{q^2} + \frac{3h_{uvv}}{q} + \left[\frac{h_{uuu}(1-\omega_0^2)}{q^3} + \frac{2h_{uuv}}{q^2} + \frac{h_{uvv}}{q}\right]\omega_0 \mathrm{i},
\end{aligned}$$

with

$$\begin{aligned}
&g_{uu} = -2\gamma + \frac{2h\chi_0^H}{p+hu^*+mv^*}, \ g_{uuu} = -\frac{6h^2\chi_0^H}{(p+hu^*+mv^*)^2}, \quad h_{uu} = -\frac{2q^2}{(1+qu^*)},\\
&g_{uv} = -\left(\frac{\theta K}{(1+Kv^*)^2} + \frac{(p^2+hpu^*+pmv^{*2}+2hmu^*v^*)}{(p+hu^*+mv^*)^3}\right), \quad h_{uv} = \frac{q}{(1+qu^*)},\\
&g_{vv} = \frac{2\theta K^2 u^*}{(1+Kv^*)^3} + \frac{2mu^*(p+hu^*)\chi_0^H}{v^*(p+mv^*)(p+hu^*+mv^*)}, \quad h_{vv} = -\frac{2}{1+qu^*},\\
&g_{uuv} = \frac{2h(p^2+hpu^*-m^2v^{*2}+2hmu^*v^*)}{(p+hu^*+mv^*)^4}, \quad h_{uuu} = \frac{6q^3}{(1+qu^*)^2},\\
&g_{uvv} = \frac{2\theta K^2}{(1+Kv^*)^3} + \frac{2m(p^2-h^2u^{*2}+mpv^*+2hmu^*v^*)}{(p+hu^*+mv^*)^4}, \quad h_{uuv} = -\frac{2q^2}{(1+qu^*)^2},\\
&g_{vvv} = -\left(\frac{6\theta K^3 u^*}{(1+Kv^*)^4} + \frac{6m^2u^*(p+hu^*)\chi_0^H}{v^*(p+mv^*)(p+hu^*+mv^*)^2}\right), \quad h_{uvv} = \frac{2q}{(1+qu^*)^2}.
\end{aligned}$$

Then, through straightforward calculations, we can get that

$$\begin{aligned}
\langle \mathfrak{q}^*, \mathcal{E}_{\mathfrak{q}\mathfrak{q}} \rangle =& g_{uu} + g_{uv} + \frac{h_{vv}}{2} + \frac{h_{uu}(1-\omega_0^2-2q)}{2q^2} - \frac{1}{2\omega_0}\Big[2g_{uv} + qg_{vv} - h_{vv} \\
& - \frac{h_{uu}(1-\omega_0^2)}{q^2} + \frac{g_{uu}(1-\omega_0^2) - 2h_{uu}\omega_0^2 - 2h_{uv}(1+\omega_0^2)}{q}\Big]\mathrm{i}, \\
\langle \mathfrak{q}^*, \mathcal{E}_{\mathfrak{q}\bar{\mathfrak{q}}} \rangle =& \frac{h_{vv}}{2} + \frac{h_{uu}(1-\omega_0^2)}{2q^2} + \frac{h_{uv}}{q} \\
& - \frac{1}{2\omega_0}\Big[2g_{uv} + qg_{vv} - h_{vv} - \frac{h_{uu}(1-\omega_0^2)}{q^2} + \frac{g_{uu}(1-\omega_0^2) - 2h_{uv}}{q}\Big]\mathrm{i}, \\
\langle \mathfrak{q}^*, \mathcal{J}_{\mathfrak{q}\mathfrak{q}\bar{\mathfrak{q}}} \rangle =& -\Big[\frac{g_{uvv}}{2} + \frac{g_{uuu}(1-\omega_0^2) - h_{uuv}(1-3\omega_0^2)}{2q^2} + \frac{g_{uuv} - h_{uvv}}{q}\Big] \\
& + \frac{1}{2\omega_0}\Big[3g_{uvv} + qg_{vvv} + \frac{h_{uuu}}{q^3} + \frac{g_{uuu}(1-\omega_0^2) + h_{uuv}(3-\omega_0^2)}{q^2} \\
& + \frac{3g_{uuv}(1-\omega_0^2) + h_{uvv}(3+\omega_0^2)}{q}\Big]\mathrm{i}.
\end{aligned}$$

According to [25], we have

$$\begin{aligned}
\mathrm{Re}(c_1(\chi_0^H)) =& \mathrm{Re}\left(\frac{\mathrm{i}}{2\omega_0}\left(f_{20}f_{11} - 2|f_{11}|^2 - \frac{|f_{02}|^2}{3}\right) + \frac{f_{21}}{2}\right) \\
=& \mathrm{Re}\left(\frac{\mathrm{i}}{2\omega_0}\langle \mathfrak{q}^*, \mathcal{E}_{\mathfrak{q}\mathfrak{q}} \rangle \cdot \langle \mathfrak{q}^*, \mathcal{E}_{\mathfrak{q}\bar{\mathfrak{q}}} \rangle + \frac{1}{2}\langle \mathfrak{q}^*, \mathcal{J}_{\mathfrak{q}\mathfrak{q}\bar{\mathfrak{q}}} \rangle\right) \\
=& \frac{1}{4\omega_0^2}\left[g_{uu} + g_{uv} + h_{vv} + \frac{h_{uu}(1-\omega_0^2)}{q^2} + \frac{2h_{uv} - h_{uu}}{q}\right] \\
& \times \left[2g_{uv} + qg_{vv} - h_{vv} - \frac{h_{uu}(1-\omega_0^2)}{q^2} + \frac{g_{uu}(1-\omega_0^2) - 2h_{uv}}{q}\right] \\
& - \frac{h_{uu} + h_{uv}}{4q}\left[h_{vv} + \frac{h_{uu}(1-\omega_0^2)}{q^2} + \frac{2h_{uv}}{q}\right] \\
& - \frac{1}{4}\Big[g_{uvv} + \frac{g_{uuu}(1-\omega_0^2) - h_{uuv}(1-3\omega_0^2)}{q^2} + \frac{2(g_{uuv} - h_{uvv})}{q}\Big].
\end{aligned}$$

From (3.7), we have $\rho'(\chi) < 0$, then the sign of $\mathrm{Re}(c_1(\chi_0^H))$ can determine the direction and stability of Hopf bifurcation periodic solutions. □

Theorem 3.5. *Assume the conditions of Theorem 3.3 are satisfied, the bifurcating periodic solutions of spatial inhomogeneous are stable (unstable), and the direction is subcritical (supercritical) when* $\mathrm{Re}(c_1(\chi_j^H)) < 0 (> 0)$.

Proof. Let

$$\begin{aligned}
\mathfrak{q} &= \left(\mathfrak{a}_j, \mathfrak{b}_j\right)^T \cos\frac{j}{l}x = \left(\frac{1}{q}\left(1 + d_2\frac{j^2}{l^2} + \omega_j\mathrm{i}\right), 1\right)^T \cos\frac{j}{l}x, \\
\mathfrak{q}^* &= \left(\mathfrak{a}_j^*, \mathfrak{b}_j^*\right)^T \cos\frac{j}{l}x = \left(\frac{q}{\omega_j l\pi}\mathrm{i}, \frac{1}{l\pi} - \left(\frac{d_2 j^2}{\omega_j l^3\pi} + \frac{1}{\omega_j l\pi}\right)\mathrm{i}\right)^T \cos\frac{j}{l}x,
\end{aligned}$$

where $\omega_j = \sqrt{-1 + qb_{12}(\chi_j^H) - 2d_2\frac{j^2}{l^2} - d_2^2\frac{j^4}{l^4}}$, which satisfies $P(\chi_j)\mathfrak{q} = \omega_j\mathfrak{q}\mathrm{i}$, $P^*(\chi_j^H)\mathfrak{q}^* = -\omega\mathfrak{q}^*\mathrm{i}$, $\langle\mathfrak{q}^*, \mathfrak{q}\rangle = 1$, and $\langle\mathfrak{q}^*, \overline{\mathfrak{q}}\rangle = 0$.

From [25], we obtain that

$$\mathcal{E}_{\mathfrak{q}\mathfrak{q}} = \left(\mathfrak{c}_j, \mathfrak{d}_j\right)^T \cos^2\frac{j}{l}x,\ \mathcal{E}_{\mathfrak{q}\bar{\mathfrak{q}}} = \left(\mathfrak{e}_j, \mathfrak{f}_j\right)^T \cos^2\frac{j}{l}x,\ \mathcal{J}_{\mathfrak{q}\mathfrak{q}\bar{\mathfrak{q}}} = \left(\mathfrak{g}_j, \mathfrak{h}_j\right)^T \cos^3\frac{j}{l}x,$$

where

$$\begin{aligned}
\mathfrak{c}_j =& \frac{g_{uu}}{q^2}\left[\left(1 + d_2\frac{j^2}{l^2}\right)^2 - \omega_j^2\right] + \frac{2g_{uv}}{q}\left(1 + d_2\frac{j^2}{l^2}\right) + g_{vv} + \frac{2\omega_j}{q}\left[\frac{g_{uu}}{q}\left(1 + d_2\frac{j^2}{l^2}\right) + g_{uv}\right]\mathrm{i},\\
\mathfrak{d}_j =& \frac{h_{uu}}{q^2}\left[\left(1 + d_2\frac{j^2}{l^2}\right)^2 - \omega_j^2\right] + \frac{2h_{uv}}{q}\left(1 + d_2\frac{j^2}{l^2}\right) + h_{vv} + \frac{2\omega_j}{q}\left[\frac{h_{uu}}{q}\left(1 + d_2\frac{j^2}{l^2}\right) + h_{uv}\right]\mathrm{i},\\
\mathfrak{e}_j =& \frac{g_{uu}}{q^2}\left[\left(1 + d_2\frac{j^2}{l^2}\right)^2 - \omega_j^2\right] + \frac{2g_{uv}}{q}\left(1 + d_2\frac{j^2}{l^2}\right) + g_{vv},\\
\mathfrak{f}_j =& \frac{h_{uu}}{q^2}\left[\left(1 + d_2\frac{j^2}{l^2}\right)^2 - \omega_j^2\right] + \frac{2h_{uv}}{q}\left(1 + d_2\frac{j^2}{l^2}\right) + h_{vv},\\
\mathfrak{g}_j =& \frac{g_{uuu}}{q^3}\left(1 + d_2\frac{j^2}{l^2}\right)\left[\left(1 + d_2\frac{j^2}{l^2}\right)^2 - \omega_j^2\right] + \frac{3g_{uuv}}{q^2}\left[\left(1 + d_2\frac{j^2}{l^2}\right)^2 - \omega_j^2\right] + g_{vvv}\\
&+ \frac{3g_{uvv}}{q}\left(1 + d_2\frac{j^2}{l^2}\right) + \frac{\omega_j}{q}\left(\frac{g_{uuu}}{q^2}\left[\left(1 + d_2\frac{j^2}{l^2}\right)^2 - \omega_j^2\right] + \frac{2g_{uuv}}{q}\left(1 + d_2\frac{j^2}{l^2}\right) + 3g_{uvv}\right)\mathrm{i},\\
\mathfrak{h}_j =& \frac{h_{uuu}}{q^3}\left(1 + d_2\frac{j^2}{l^2}\right)\left[\left(1 + d_2\frac{j^2}{l^2}\right)^2 - \omega_j^2\right] + \frac{3h_{uuv}}{q^2}\left[\left(1 + d_2\frac{j^2}{l^2}\right)^2 - \omega_j^2\right]\\
&+ \frac{3h_{uvv}}{q}\left(1 + d_2\frac{j^2}{l^2}\right) + \frac{\omega_j}{q}\left(\frac{h_{uuu}}{q^2}\left[\left(1 + d_2\frac{j^2}{l^2}\right)^2 - \omega_j^2\right] + \frac{2h_{uuv}}{q}\left(1 + d_2\frac{j^2}{l^2}\right) + 3h_{uvv}\right)\mathrm{i},
\end{aligned}$$

with

$$\begin{aligned}
&g_{uu} = -2\gamma + \frac{2h\chi_j^H}{p + hu^* + mv^*},\ g_{uuu} = -\frac{6h^2\chi_j^H}{(p + hu^* + mv^*)^2}, \quad h_{uu} = -\frac{2q^2}{1 + qu^*},\\
&g_{uv} = -\left(\frac{\theta K}{(1 + Kv^*)^2} + \frac{(p^2 + hpu^* + pmv^{*2} + 2hmu^*v^*)}{(p + hu^* + mv^*)^3}\right), \quad h_{uv} = \frac{q}{1 + qu^*},\\
&g_{vv} = \frac{2\theta K^2u^*}{(1 + Kv^*)^3} + \frac{2mu^*(p + hu^*)\chi_j^H}{v^*(p + mv^*)(p + hu^* + mv^*)}, \quad h_{vv} = -\frac{2}{1 + qu^*},\\
&g_{uuv} = \frac{2h(p^2 + hpu^* - m^2v^{*2} + 2hmu^*v^*)}{(p + hu^* + mv^*)^4}, \quad h_{uuu} = \frac{6q^3}{(1 + qu^*)^2},\\
&g_{uvv} = \frac{2\theta K^2}{(1 + Kv^*)^3} + \frac{2m(p^2 - h^2u^{*2} + mpv^* + 2hmu^*v^*)}{(p + hu^* + mv^*)^4}, \quad h_{uuv} = -\frac{2q^2}{(1 + qu^*)^2},
\end{aligned}$$

$$g_{vvv} = -\left(\frac{6\theta K^3u^*}{(1 + Kv^*)^4} + \frac{6m^2u^*(p + hu^*)\chi_j^H}{v^*(p + mv^*)(p + hu^* + mv^*)^2}\right), \quad h_{uvv} = \frac{2q}{(1 + qu^*)^2}.$$

According to [25], we have

$$[(2\omega_j \mathrm{i} I - P_{2j}(\chi_j^H))]^{-1} = \frac{\varsigma_1 - \varsigma_2 \mathrm{i}}{\varsigma_1^2 + \varsigma_2^2} \begin{pmatrix} 2\omega_j \mathrm{i} + 4d_2 \frac{j^2}{l^2} + 1 & -b_{12}(\chi_j^H) \\ q & 2\omega_j \mathrm{i} + (3d_1 - d_2)\frac{j^2}{l^2} - 1 \end{pmatrix},$$
$$[(2\omega_j \mathrm{i} I - P_0(\chi_j^H))]^{-1} = \frac{\varsigma_3 - \varsigma_4 \mathrm{i}}{\varsigma_3^2 + \varsigma_4^2} \begin{pmatrix} 2\omega_j \mathrm{i} + 1 & -b_{12}(\chi_j^H) \\ q & 2\omega_j \mathrm{i} - (d_1 + d_2)\frac{j^2}{l^2} - 1 \end{pmatrix},$$

where

$$\varsigma_1 = 3d_2(4d_1 - d_2)\frac{j^4}{l^4} + 3(d_1 - d_2)\frac{j^2}{l^2} - 3\omega_j^2, \quad \varsigma_2 = 6\omega_j(d_1 + d_2)\frac{j^2}{l^2},$$
$$\varsigma_3 = d_2^2\frac{j^4}{l^4} - (d_1 - d_2)\frac{j^2}{l^2} - 3\omega_j^2, \qquad \varsigma_4 = -2\omega_j(d_1 + d_2)\frac{j^2}{l^2}.$$

Then, we have

$$\begin{aligned} w_{20} =& \frac{1}{2}\left([(2\omega_j \mathrm{i} I - P_{2j}(\chi_j^H))]^{-1}\cos\frac{2j}{l}x + [(2\omega_j \mathrm{i} I - P_0(\chi_j^H))]^{-1}\right)\cdot \begin{pmatrix} \mathfrak{c}_j \\ \mathfrak{d}_j \end{pmatrix} \\ =& \frac{\varsigma_1 - \varsigma_2 \mathrm{i}}{2(\varsigma_1^2 + \varsigma_2^2)} \begin{pmatrix} \left(2\omega_j \mathrm{i} + 4d_2\frac{j^2}{l^2} + 1\right)\mathfrak{c}_j - b_{12}(\chi_j^H)\mathfrak{d}_j \\ q\mathfrak{c}_j + \left(2\omega_j \mathrm{i} + (3d_1 - d_2)\frac{j^2}{l^2} - 1\right)\mathfrak{d}_j \end{pmatrix}\cos\frac{2j}{l}x \\ &+ \frac{\varsigma_3 - \varsigma_4 \mathrm{i}}{2(\varsigma_3^2 + \varsigma_4^2)} \begin{pmatrix} (2\omega_j \mathrm{i} + 1)\mathfrak{c}_j - b_{12}(\chi_j^H)\mathfrak{d}_j \\ q\mathfrak{c}_j + \left(2\omega_j \mathrm{i} - (d_1 + d_2)\frac{j^2}{l^2} - 1\right)\mathfrak{d}_j \end{pmatrix}. \end{aligned}$$

Since

$$[(-P_{2j}(\chi_j^H))]^{-1} = \frac{1}{\varsigma_5} \begin{pmatrix} 4d_2\frac{j^2}{l^2} + 1 & -b_{12}(\chi_j^H) \\ q & (3d_1 - d_2)\frac{j^2}{l^2} - 1 \end{pmatrix},$$
$$[(-P_0(\chi_j^H))]^{-1} = \frac{1}{\varsigma_6} \begin{pmatrix} 1 & -b_{12}(\chi_j^H) \\ q & -(d_1 + d_2)\frac{j^2}{l^2} - 1 \end{pmatrix},$$

where

$$\varsigma_5 = 3d_2(4d_1 - d_2)\frac{j^4}{l^4} + 3(d_1 - d_2)\frac{j^2}{l^2} + \omega_j^2, \ \varsigma_6 = d_2^2\frac{j^4}{l^4} - (d_1 - d_2)\frac{j^2}{l^2} + \omega_j^2.$$

Then, we get

$$\begin{aligned} w_{11} =& \frac{1}{2}\left([-P_{2j}(\chi_j^H)]^{-1}\cos\frac{2j}{l}x + [-P_0(\chi_j^H)]^{-1}\right)\cdot \begin{pmatrix} \mathfrak{e}_j \\ \mathfrak{f}_j \end{pmatrix} \\ =& \frac{1}{2\varsigma_5} \begin{pmatrix} \left(4d_2\frac{j^2}{l^2} + 1\right)\mathfrak{e}_j - b_{12}(\chi_j^H)\mathfrak{f}_j \\ q\mathfrak{e}_j + \left((3d_1 - d_2)\frac{j^2}{l^2} - 1\right)\mathfrak{f}_j \end{pmatrix}\cos\frac{2j}{l}x \\ &+ \frac{1}{2\varsigma_6} \begin{pmatrix} \mathfrak{e}_j - b_{12}(\chi_j^H)\mathfrak{f}_j \\ q\mathfrak{e}_j - \left((d_u + d_v)\frac{j^2}{l^2} + 1\right)\mathfrak{f}_j \end{pmatrix}. \end{aligned}$$

Then,

$$\begin{aligned}\mathcal{E}_{w_{20}q} =& \begin{pmatrix} g_{uu}\bar{\mathfrak{a}}_j\tilde{\xi} + g_{uv}(\bar{\mathfrak{a}}_j\tilde{\zeta} + \tilde{\xi}) + g_{vv}\tilde{\zeta} \\ h_{uu}\bar{\mathfrak{a}}_j\tilde{\xi} + h_{uv}(\bar{\mathfrak{a}}_j\tilde{\zeta} + \tilde{\xi}) + h_{vv}\tilde{\zeta} \end{pmatrix}\cos\frac{2j}{l}x\cos\frac{j}{l}x \\ &+ \begin{pmatrix} g_{uu}\bar{\mathfrak{a}}_j\tilde{\gamma} + g_{uv}(\bar{\mathfrak{a}}_j\tilde{\chi} + \tilde{\gamma}) + g_{vv}\tilde{\chi} \\ h_{uu}\bar{\mathfrak{a}}_j\tilde{\gamma} + h_{uv}(\bar{\mathfrak{a}}_j\tilde{\chi} + \tilde{\gamma}) + h_{vv}\tilde{\chi} \end{pmatrix}\cos\frac{j}{l}x, \\ \mathcal{E}_{w_{11}q} =& \begin{pmatrix} g_{uu}\mathfrak{a}_j\bar{\xi} + g_{uv}(\mathfrak{a}_j\bar{\zeta} + \bar{\xi}) + g_{vv}\bar{\zeta} \\ h_{uu}\mathfrak{a}_j\bar{\xi} + h_{uv}(\mathfrak{a}_j\bar{\zeta} + \bar{\xi}) + h_{vv}\bar{\zeta} \end{pmatrix}\cos\frac{2j}{l}x\cos\frac{j}{l}x \\ &+ \begin{pmatrix} g_{uu}\mathfrak{a}_j\bar{\gamma} + g_{uv}(\mathfrak{a}_j\bar{\chi} + \bar{\gamma}) + g_{vv}\bar{\chi} \\ h_{uu}\mathfrak{a}_j\bar{\gamma} + h_{uv}(\mathfrak{a}_j\bar{\chi} + \bar{\gamma}) + h_{vv}\bar{\chi} \end{pmatrix}\cos\frac{j}{l}x, \end{aligned}$$

where

$$\begin{aligned}\tilde{\xi} =& \frac{\varsigma_1 - \varsigma_2\mathrm{i}}{2(\varsigma_1^2 + \varsigma_2^2)}\left[\left(2\omega_j\mathrm{i} + 4d_2\frac{j^2}{l^2} + 1\right)\mathfrak{c}_j - b_{12}(\chi_j^H)\mathfrak{d}_j\right], \\ \tilde{\zeta} =& \frac{\varsigma_1 - \varsigma_2\mathrm{i}}{2(\varsigma_1^2 + \varsigma_2^2)}\left[q\mathfrak{c}_j + \left(2\omega_j\mathrm{i} + (3d_1 - d_2)\frac{j^2}{l^2} - 1\right)\mathfrak{d}_j\right], \\ \tilde{\gamma} =& \frac{\varsigma_3 - \varsigma_4\mathrm{i}}{2(\varsigma_3^2 + \varsigma_4^2)}\left[(2\omega_j\mathrm{i} + 1)\mathfrak{c}_j - b_{12}(\chi_j^H)\mathfrak{d}_j\right], \\ \tilde{\chi} =& \frac{\varsigma_3 - \varsigma_4\mathrm{i}}{2(\varsigma_3^2 + \varsigma_4^2)}\left[q\mathfrak{c}_j + \left(2\omega_j\mathrm{i} - (d_1 + d_2)\frac{j^2}{l^2} - 1\right)\mathfrak{d}_j\right], \\ \bar{\xi} =& \frac{1}{2\varsigma_5}\left[\left(4d_2\frac{j^2}{l^2} + 1\right)\mathfrak{e}_j - b_{12}(\chi_j^H)\mathfrak{f}_j\right], \\ \bar{\zeta} =& \frac{1}{2\varsigma_5}\left[q\mathfrak{e}_j + \left((3d_1 - d_2)\frac{j^2}{l^2} - 1\right)\mathfrak{f}_j\right], \\ \bar{\gamma} =& \frac{1}{2\varsigma_6}\left[\mathfrak{e}_j - b_{12}(\chi_j^H)\mathfrak{f}_j\right], \\ \bar{\chi} =& \frac{1}{2\varsigma_6}\left[q\mathfrak{e}_j - \left((d_u + d_v)\frac{j^2}{l^2} + 1\right)\mathfrak{f}_j\right]. \end{aligned}$$

Note that

$$\begin{aligned}&\int_0^{l\pi}\cos^2\frac{j}{l}x\mathrm{d}x = \frac{l\pi}{2}, \quad \int_0^{l\pi}\left(\cos\frac{2j}{l}x\cos^2\frac{j}{l}x\right)\mathrm{d}x = \frac{l\pi}{4}, \\ &\int_0^{l\pi}\cos^3\frac{j}{l}x\mathrm{d}x = 0, \quad \int_0^{l\pi}\cos^4\frac{j}{l}x\mathrm{d}x = \frac{3l\pi}{8}. \end{aligned}$$

Thus

$$\begin{aligned}\langle\mathfrak{q}^*, \mathcal{E}_{\mathfrak{q}\mathfrak{q}}\rangle =& \langle\mathfrak{q}^*, \mathcal{E}_{\mathfrak{q}\bar{\mathfrak{q}}}\rangle = 0,\ \langle\mathfrak{q}^*, \mathcal{J}_{\mathfrak{q}\mathfrak{q}\bar{\mathfrak{q}}}\rangle = \frac{3l\pi}{8}(\mathfrak{g}_j\bar{\mathfrak{a}}_j^* + \mathfrak{h}_j\bar{\mathfrak{b}}_j^*), \\ \langle\mathfrak{q}^*, \mathcal{E}_{w_{20}\bar{\mathfrak{q}}}\rangle =& \frac{l\pi}{4}[\bar{\mathfrak{a}}_j^*(g_{uu}\bar{\mathfrak{a}}_j\tilde{\xi} + g_{uv}(\bar{\mathfrak{a}}_j\tilde{\zeta} + \tilde{\xi}) + g_{vv}\tilde{\zeta}) + \bar{\mathfrak{b}}_j^*(h_{uu}\bar{\mathfrak{a}}_j\tilde{\xi} + h_{uv}(\bar{\mathfrak{a}}_j\tilde{\zeta} + \tilde{\xi}) + h_{vv}\tilde{\zeta})] \\ &+ \frac{l\pi}{2}[\bar{\mathfrak{a}}_j^*(g_{uu}\bar{\mathfrak{a}}_j\tilde{\gamma} + g_{uv}(\bar{\mathfrak{a}}_j\tilde{\chi} + \tilde{\gamma}) + g_{vv}\tilde{\chi}) + \bar{\mathfrak{b}}_j^*(h_{uu}\bar{\mathfrak{a}}_j\tilde{\gamma} + h_{uv}(\bar{\mathfrak{a}}_j\tilde{\chi} + \tilde{\gamma}) + h_{vv}\tilde{\chi})], \\ \langle\mathfrak{q}^*, \mathcal{E}_{w_{11}\mathfrak{q}}\rangle =& \frac{l\pi}{4}[\bar{\mathfrak{a}}_j^*(g_{uu}\mathfrak{a}_j\bar{\xi} + g_{uv}(\mathfrak{a}_j\bar{\zeta} + \bar{\xi}) + g_{vv}\bar{\zeta}) + \bar{\mathfrak{b}}_j^*(h_{uu}\mathfrak{a}_j\bar{\xi} + h_{uv}(\mathfrak{a}_j\bar{\zeta} + \bar{\xi}) + h_{vv}\bar{\zeta})] \\ &+ \frac{l\pi}{2}[\bar{\mathfrak{a}}_j^*(g_{uu}\mathfrak{a}_j\bar{\gamma} + g_{uv}(\mathfrak{a}_j\bar{\chi} + \bar{\gamma}) + g_{vv}\bar{\chi}) + \bar{\mathfrak{b}}_j^*(h_{uu}\mathfrak{a}_j\bar{\gamma} + h_{uv}(\mathfrak{a}_j\bar{\chi} + \bar{\gamma}) + h_{vv}\bar{\chi})]. \end{aligned}$$

According to [25], we have

$$\begin{aligned}\mathrm{Re}(c_1(\chi_j^H)) =&\mathrm{Re}\left(\frac{\mathrm{i}}{2\omega_0}\langle \mathfrak{q}^*, \mathcal{E}_{\mathfrak{q}\mathfrak{q}}\rangle \cdot \langle \mathfrak{q}^*, \mathcal{E}_{\mathfrak{q}\bar{\mathfrak{q}}}\rangle + \langle \mathfrak{q}^*, \mathcal{E}_{w_{11}\mathfrak{q}}\rangle + \frac{1}{2}\langle \mathfrak{q}^*, \mathcal{E}_{w_{20}\bar{\mathfrak{q}}}\rangle + \frac{1}{2}\langle \mathfrak{q}^*, \mathcal{J}_{\mathfrak{q}\mathfrak{q}\bar{\mathfrak{q}}}\rangle\right)\\ =&\mathrm{Re}\langle \mathfrak{q}^*, \mathcal{E}_{w_{11}\mathfrak{q}}\rangle + \frac{1}{2}\mathrm{Re}\langle \mathfrak{q}^*, \mathcal{E}_{w_{20}\bar{\mathfrak{q}}}\rangle + \frac{1}{2}\mathrm{Re}\langle \mathfrak{q}^*, \mathcal{J}_{\mathfrak{q}\mathfrak{q}\bar{\mathfrak{q}}}\rangle.\end{aligned}$$

From (3.7), we have $\rho'(\chi) < 0$, then the direction and stability of the periodic solution of Hopf bifurcation can be determined by the sign of $\mathrm{Re}(c_1(\chi_j^H))$. □

4. Numerical simulations

We perform a series of numerical simulation on models (1.3) and (1.4) to illustrate our results. Let initial values $(u(0), v(0)) = (2, 3)$ and parameter values in Table 2. Then, we obtain that $R_0 = 4.6 > 0$, $\theta^* = 2.1833 > \theta = 1.2$, $\chi = 0.6467 < \chi^* = 1.4034$, which imply that model (1.3) has a stable node $E_2(23, 0)$, an unstable positive equilibrium $E^*(u^*, v^*) = (4.1418, 5.9701)$, and a stable limit cycle (see Figure 4). When $\theta = 4$, we have $\theta^* = 2.1833 < \theta = 4$ and $\chi = 0.5132 > \chi^* = 0.4843$, which imply that a stable node $E_2(23, 0)$ becomes an unstable and the unstable equilibrium becomes $E^*(u^*, v^*) = (7.1403, 9.5684)$ which is stable; moreover, the limit cycle is disappears (see Figure 5).

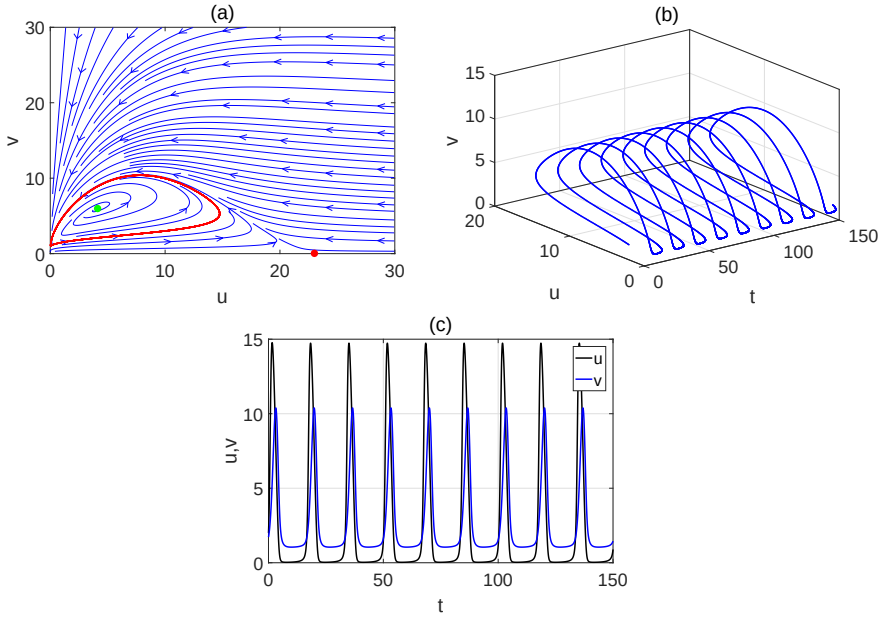

Figure 4. Phase portrait and time sequence diagram of model (1.3). In (a), red 'o' represents stable equilibrium $E_2 = (23, 0)$ and green 'o' represents unstable equilibrium $E^*(u^*, v^*) = (4.1418, 5.9701)$ for $\chi = 0.6467 < \chi^* = 1.4034$; the red line represents a stable limit cycle.

Table 2. The parameter values of model (1.3).

Parameter	Value	Parameter	Value	Parameter	Value	Parameter	Value
r	3.4	γ	0.2	K	0.34	p	0.2
θ	1.2	h	0.38	m	0.04	q	1.2

According to Figures 4 and 5, we find that as $\theta(1.2 \rightarrow 4)$ increases, the positive equilibrium $E^*(u^*, v^*)$ of model (1.3) changes from unstable to stable, and the limit cycle changes from existence to nonexistence, in addition, it also led to an increase in population size. This fully demonstrates that θ can affect the stability and the population size of model (1.3).

Note that $\theta = \frac{r_0(1-\eta)}{b}$, that is, θ and η are negatively correlated. Therefore, if the minimum fear cost η is used as a key parameter to explore the dynamic behavior and the trend of populations, it can be replaced by θ. We find from Figures 6 and 7 that as θ increases, that is, as the minimum fear cost η decreases, the model (1.3) exhibits a limit cycle, which first changes from a large and stable range to a small and unstable range and gradually disappears, while the positive equilibrium gradually changes from an unstable to a globally stable. This means that a lower cost of fear can maintain population stability, causing a decrease in population size but not leading to extinction, while a higher cost of fear can disrupt stability and cause periodic changes in population size.

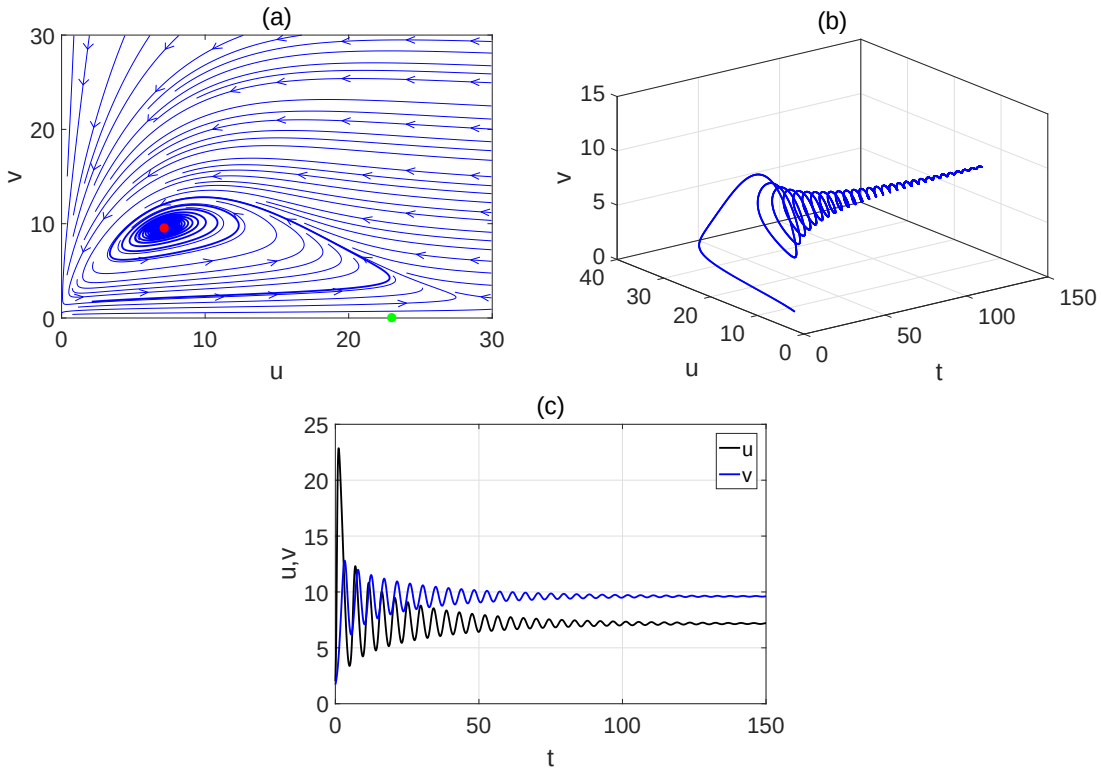

Figure 5. Phase portrait and time sequence diagram of model (1.3). In (a), green 'o' represents unstable equilibrium $E_2 = (23, 0)$ and red 'o' represents stable equilibrium $E^*(u^*, v^*) = (7.1403, 9.5684)$ for $\chi = 0.5132 > \chi^* = 0.4843$. $\theta = 4$.

We draw the bifurcation diagram of model (1.3) with the various parameters θ, r, K, h, p, q, m (see Figures 7–9) and observe that the various parameters can stabilize the oscillating model via Hopf bifurcation. It is revealed that: (i) for θ, r, m, p, the small parameter values will destroy the stability and produce Hopf bifurcation; (ii) for K, the large parameter value will destroy the stability and produce Hopf bifurcation; (iii) for h, q, the bubble phenomenon [26] appears, which means that the appropriate parameter values will destroy the stability and produce Hopf bifurcation, but the small and large parameter values cannot destroy the stability of populations. Therefore, different parameters can have an impact on the dynamic behavior of model (1.3), mainly interfering with the stability of the equilibria and the existence, stability, and direction of Hopf bifurcations.

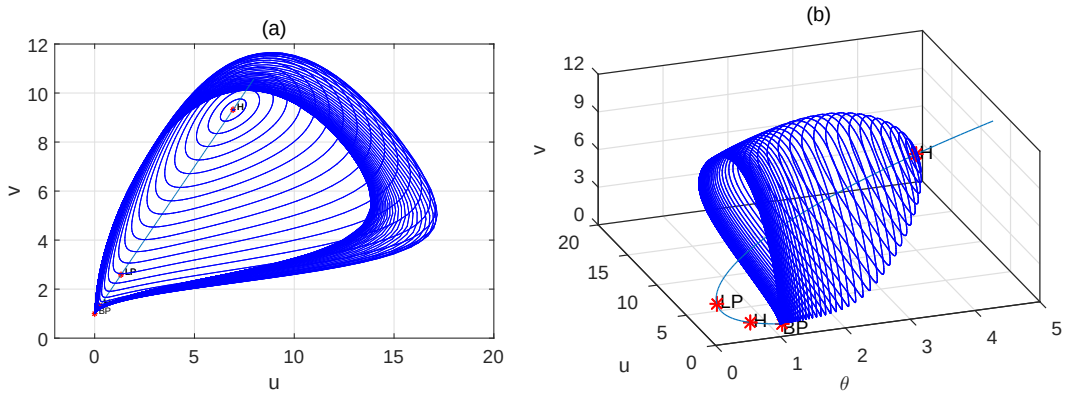

Figure 6. Bifurcation diagrams of model (1.3) in $u-v$ (left) and $\theta-u-v$ (right) parametric space. Hopf critical point H: $(u, v, \theta) = (6.9341, 9.3209, 3.7210)$, the 1st Lyapunov coefficient $= -5.1964\times10^{-3}$; LP: $(u, v, \theta) = (1.3198, 2.5838, 0.1392)$; Neutral saddle point H: $(u, v, \theta) = (0.2607, 1.3128, 0.5587)$; BP: $(u, v, \theta) = (0, 1, 1.0273)$.

For model (1.4), let initial values be $(u_0(x), v_0(x)) = (4.5297 + 0.2\sin(x), 7.0543 + 0.2\sin(x))$, $d_2 = 0.2$, $\Omega = (0, 40)$, and change the different parameter values θ and d_1 to discuss the influence of fear and diffusion rate of prey on the dynamics of model (1.4).

Let $\theta = 4$, $d_1 = 0.1$, and according to Theorem 3.1, we get that $\chi = 0.5132 > \chi^* = 0.4843$ and $-(\chi^* - \chi + 1) + 2qb_{12} - 2\sqrt{-qb_{12}(\chi^* - \chi + 1 - qb_{12})} = 0.0969 < \frac{d_1}{d_2} = 0.5 < \chi^* - \chi + 1 = 0.9711$, which imply that the steady state solution of model (1.4) is locally asymptotically stable. If d_1 is selected as 0.01 and 0.001, respectively, according to Theorem 3.1, we have

$$0 < \frac{d_1}{d_2} = 0.05 < -(\chi^* - \chi + 1) + 2qb_{12} - 2\sqrt{-qb_{12}(\chi^* - \chi + 1 - qb_{12})} = 0.0969,$$

$$0 < \frac{d_1}{d_2} = 0.005 < -(\chi^* - \chi + 1) + 2qb_{12} - 2\sqrt{-qb_{12}(\chi^* - \chi + 1 - qb_{12})} = 0.0969,$$

which imply that the Turing instability occurs. This further reflects that diffusion can lead to the occurrence of Turing patterns, providing ideas for studying the morphology of populations and effectively enriching the explosion of species diversity.

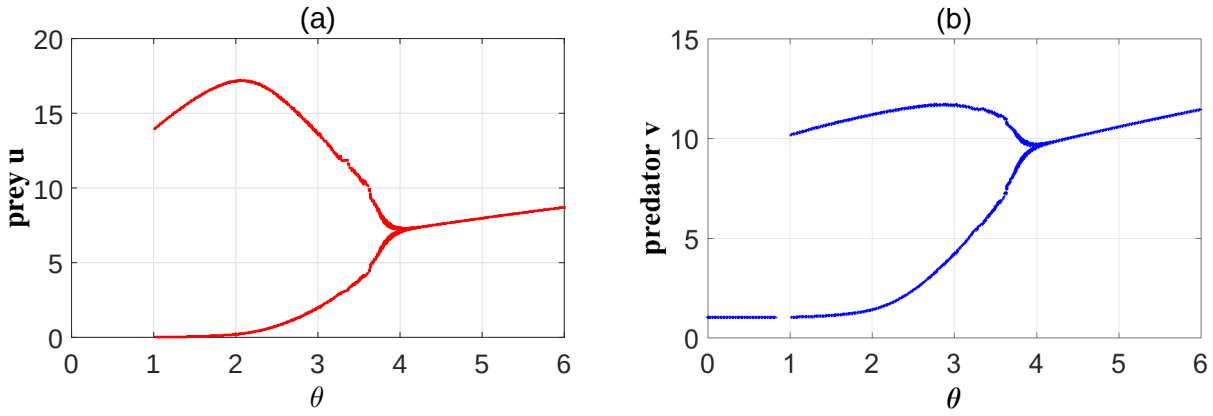

Figure 7. Bifurcation diagram shows that $\theta = \frac{r_0(1-\eta)}{b}$ can stabilize the model (1.3).

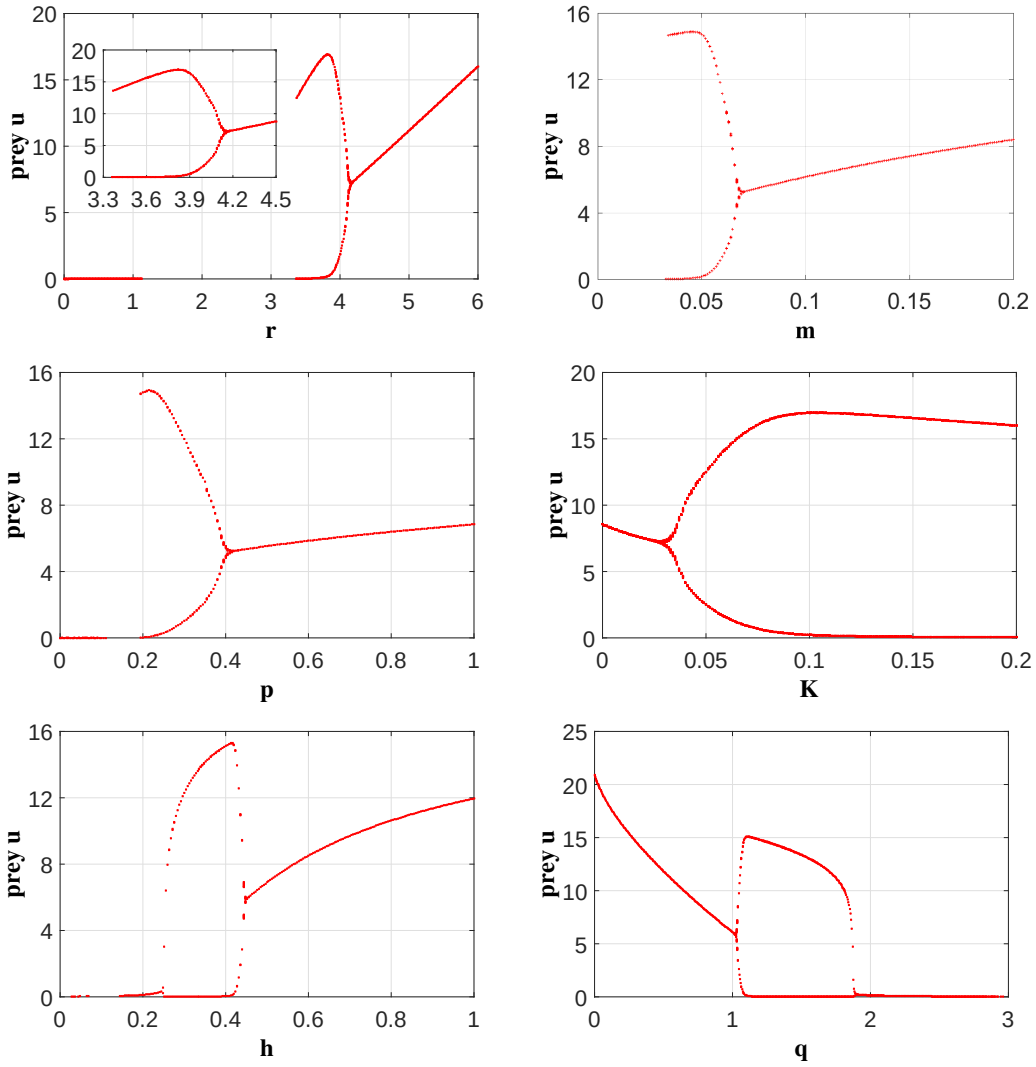

Figure 8. Bifurcation diagram for prey of model (1.3) with various parameters.

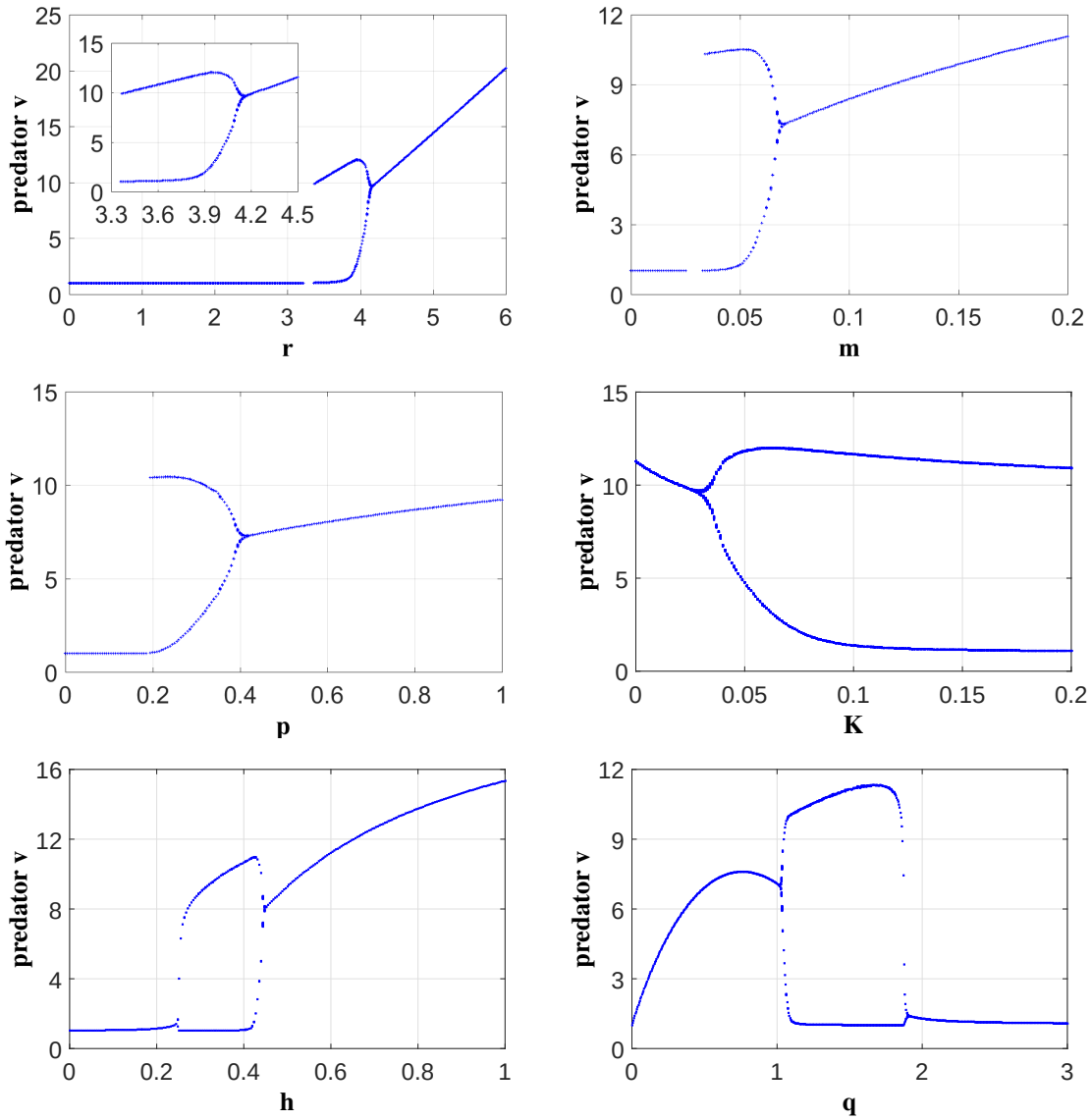

Figure 9. Bifurcation diagram for predator of model (1.3) with various parameters.

Next, select θ as 6 and 10, respectively, then we can also get that

$$\chi = 0.4793 > \chi^* = 0.1598,\ -(\chi^* - \chi + 1) + 2qb_{12} - 2\sqrt{-qb_{12}(\chi^* - \chi + 1 - qb_{12})} = 0.0403,$$

$$\chi = 0.444 > \chi^* = -0.3495,\ -(\chi^* - \chi + 1) + 2qb_{12} - 2\sqrt{-qb_{12}(\chi^* - \chi + 1 - qb_{12})} = 0.003.$$

By Theorem 3.1, the steady state solution of model (1.4) is locally asymptotically stable when $\theta = 6$ or $\theta = 10$.

By comparing Figures 10 and 11 in detail, we find that (i) the larger θ and d_1, the steady state solution of model (1.4) is more stable, indicating that the smaller the fear effect, or the larger the diffusion rate of prey (predator), the more conducive to the stability of prey (predator) population; (ii) the smaller θ and d_1, the steady state solution of model (1.4) is more unstable, indicating that the greater the fear effect, or the smaller the diffusion rate of prey, the less conducive to the stability of prey(predator) population. Thus, the conclusion of Theorem 3.1 and Remark 3.1 is verified.

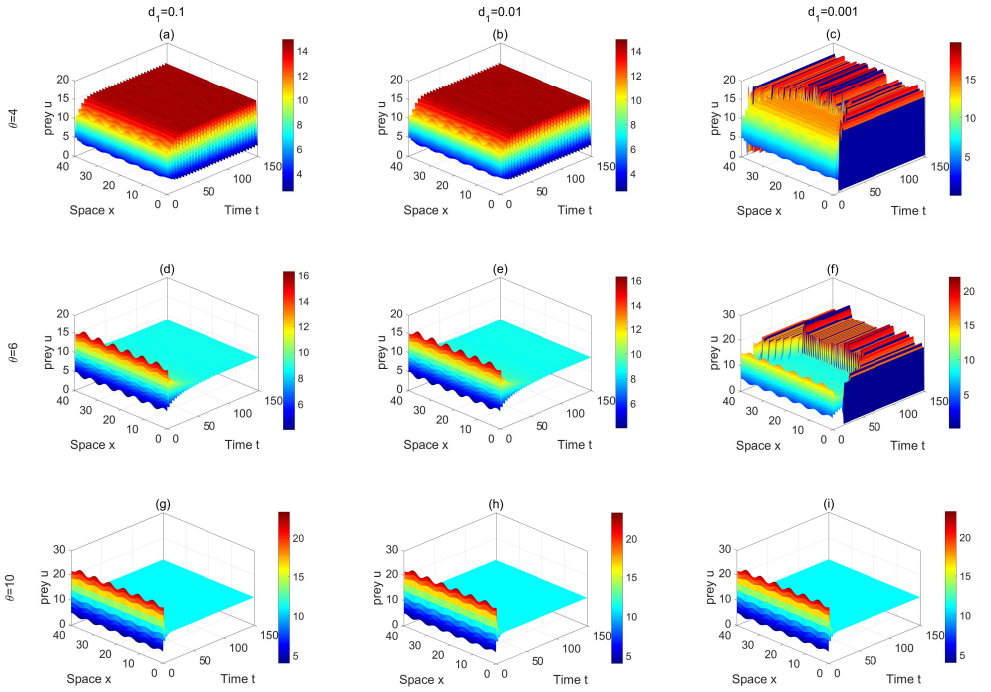

Figure 10. Spatiotemporal evolution of prey of model (1.4) with different θ and d_1. $x = 40$, $t = 150$.

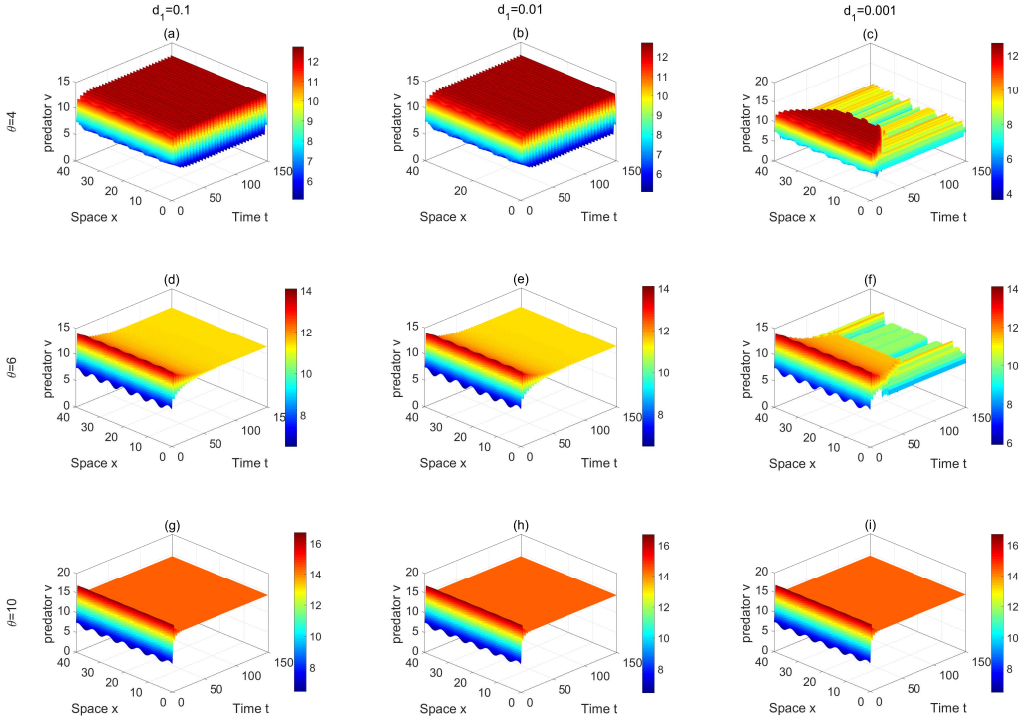

Figure 11. Spatiotemporal evolution of predator of model (1.4) with different θ and d_1. $x = 40$, $t = 150$.

In Figure 12, we give the time evolution of model (1.4) with different θ and d_1 at $x = 10$, which corresponds to Figures 10 and 11. These indicated that when the solution of model (1.4) tends to the equilibria or periodic solution, its changing form is calm; but when its changing form undergoes a big sudden change, it means that Turing instability has occurred.

In Figure 13(a)–(c), the dynamics of the solution of model (1.4) is a smooth oscillatory. In Figure 13(d), the approximations have evolved into the spatially homogeneous steady states u^* and v^*. Then, we have a conclusion that the larger θ can keep the solution of model (1.4) to the stationary distribution, while a small θ can make the solution tend to the smooth oscillatory, that is, the smaller the fear effect, the more stable the prey (predator) population will be.

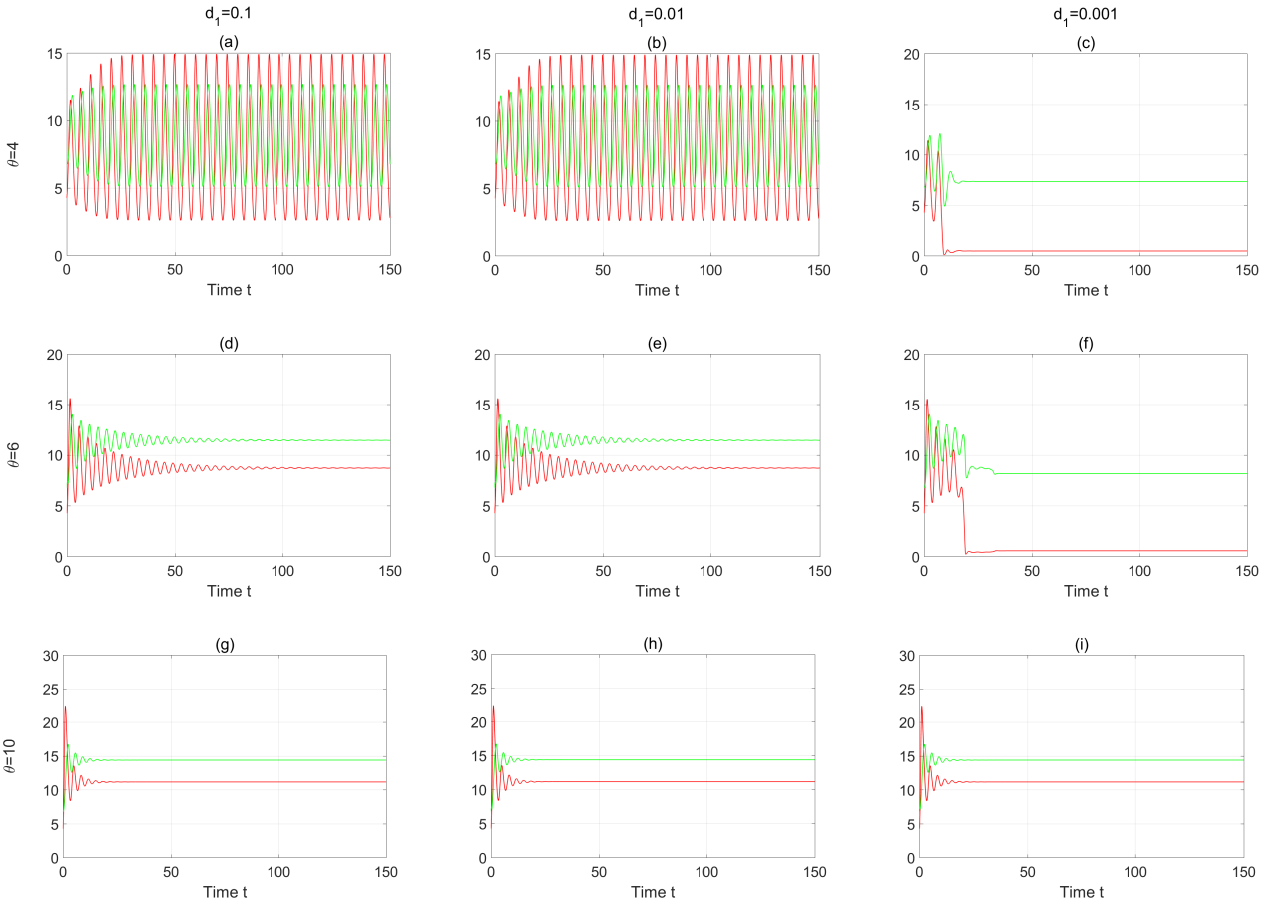

Figure 12. Time evolution diagram of model (1.4) with different θ and d_1 at $x = 10$. Red line represents prey population and green line represents predator population.

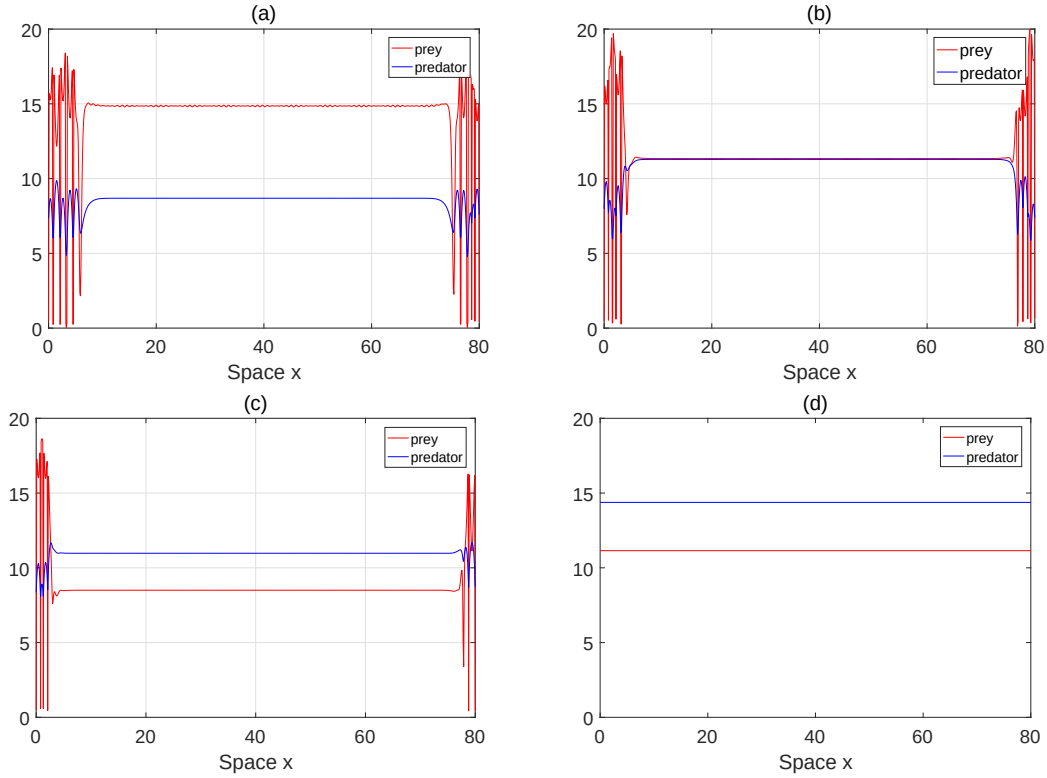

Figure 13. Numerical simulation on the dynamics of the solution of model (1.4) with different θ. $d_1 = 0.001$. $x = 80$, $t = 40$. (a): $\theta = 4$, (b): $\theta = 5$, (c): $\theta = 6$, (d): $\theta = 10$.

5. Conclusions

In this paper, a predator-prey model with B-D functional response for prey and a modified L-G functional response for predator are established to explore how fear and diffusion affect the spatiotemporal dynamics of the model. For the nonspatial model (1.3):

(1) The model exhibits rich dynamic properties. In terms of the existence of equilibrium points, the model has three boundary equilibria and at most three different positive equilibria (see Theorem 2.1 or Table 2).

(2) Discussing the local stability of the positive equilibria (see Theorems 2.2 and 2.3) and the global stability of E^* (see Theorem 2.4), which shows that under the assumption of $qb_{12} > 1$, when $\chi > \chi^*$, E^* is stable; when $\chi < \chi^*$, E^* is unstable; when $\chi = \chi^*$, the Hopf bifurcation will occur.

(3) Exploring the impact of fear on Hopf bifurcation. Fear determines the direction and stability of periodic solutions bifurcated from Hopf bifurcation that are investigated (see Theorem 2.5). The lower cost of fear facilitates the occurrence of Hopf bifurcation, leading to the emergence of limit cycles (see Figures 4–7).

(4) Our results indicate that fear can enrich and destroy the dynamic properties of the model.

For the spatial model (1.4):

(1) The diffusion of populations led to the occurrence of Turing patterns. When the ratio of the diffusion rate of prey to the diffusion rate of predator exceeds a certain critical value, Turing instability

occurs (see Theorem 3.1 and Figure 3), which favors the formation of biodiversity.

(2) Discussing the stability and direction of spatially homogeneous and inhomogeneous periodic solutions (see Theorems 3.4 and 3.5), which are mainly influenced by the decisive effects of fear and diffusion (see Figures 10–13).

(3) Our results reveal that the larger fear and lower diffusion rate of prey both can destroy the stability of populations and further promote the emergence of periodic solutions, but to a certain extent, and it is advantageous to improve the survival of the species and the formation of biodiversity.

(4) Our results enrich and develop the dynamics of predator-prey models with diffusion and different functional responses, such as the Holling II term [5, 12, 24], L-G term [27], and B-D term [13, 22].

In the future, we will continue to study the effects of fear and diffusion on the three population model, food web model, partial differential population models with cross diffusion, prey-taxis, and spatial memory. In addition, it can also study the influence of external environmental noise, impulsive, and delay on population dynamics.

Use of AI tools declaration

The authors declare they have not used Artificial Intelligence (AI) tools in the creation of this article.

Acknowledgments

This work is supported by the National Natural Science Foundation of China (Nos. 12171004, 12301616), the Doctor Research Project Foundation of Liaoning Province (No. 2023-BS-210), the Liaoning Key Laboratory of Development and Utilization for Natural Products Active Molecules (Nos. LZ202302, LZ202303), the Basic scientific research project of Liaoning Provincial Department of Education (No. JYTMS20231706), and the Doctor Research Project Foundation of Anshan Normal University (No. 23b08).

Conflict of interest

The authors declare there is no conflicts of interest.

References

1. K. B. Altendorf, J. W. Laundré, C. A. L. González, J. S. Brown, Assessing effects of predation risk on foraging behavior of mule deer, *J. Mammal.*, **82** (2001), 430–439.
2. S. Creel, D. Christianson, S. Liley, J. A. Winnie, Predation risk affects reproductive physiology and demography of Elk, *Science*, **315** (2007), 960. https://doi.org/10.1126/science.1135918
3. W. Cresswell, Predation in bird populations, *J. Ornithol.*, **152** (2011), 251–263. https://doi.org/10.1007/s10336-010-0638-1
4. L. Y. Zanette, A. F. White, M. C. Allen, M. Clinchy, Perceived predation risk reduces the number of offspring songbirds produce per year, *Science*, **334** (2011), 1398–1401. https://doi.org/10.1126/science.1210908

5. K. Sarkara, S. Khajanchi, Impact of fear effect on the growth of prey in a predator-prey interaction model, *Ecol. Complexity*, **42** (2020), 100826. https://doi.org/10.1016/j.ecocom.2020.100826
6. C. S. Holling, The functional response of invertebrate predators to prey density, *Mem. Entomol. Soc. Can.*, **98** (1966), 5–86. https://doi.org/10.4039/entm9848fv
7. J. R. Beddington, Mutual interference between parasites or predators and its effect on searching efficiency, *J. Anim. Ecol.*, **44** (1975), 331–340. https://doi.org/10.2307/3866
8. D. L. DeAngelis, R. A. Goldstein, R. V. O'neill, A model for tropic interaction, *Ecology*, **56** (1975), 881–892. https://doi.org/10.2307/1936298
9. P. H. Leslie, J. G. Gower, The properties of a stochastic model for the predator-prey type of interaction between two species, *Biometrika*, **47** (1960), 219–234. https://doi.org/10.2307/2333294
10. J. Huang, X. Xia, X. Zhang, S. Ruan, Bifurcation of Codimension 3 in a Predator-Prey System of Leslie Type with Simplified Holling Type IV Functional Response, *Int. J. Bifurcation Chaos*, **26** (2016), 1650034. https://doi.org/10.1142/S0218127416500346
11. W. Ko, K. Ryu, Qualitative analysis of a predator-prey model with Holling type II functional response incorporating a prey refuge, *J. Differ. Equations*, **231** (2006), 534–550. https://doi.org/10.1016/j.jde.2006.08.001
12. X. Wang, L. Zanette, X. Zou, Modelling the fear effect in predator-prey interactions, *J. Math. Biol.*, **73** (2016), 1179–1204. https://doi.org/10.1007/s00285-016-0989-1
13. S. Pal, S. Majhi, S. Mandal, N. Pal, Role of fear in a predator-prey model with Beddington-Deangelis functional response, *Z. Naturforsch. A*, **74** (2019), 581–595. https://doi.org/10.1515/zna-2018-0449
14. J. Wang, Y. Cai, S. Fu, W. Wang, The effect of the fear factor on the dynamics of a predator-prey model incorporating the prey refuge, *Chaos*, **29** (2019), 083109. https://doi.org/10.1063/1.5111121
15. A. M. Turing, The chemical basis of morphogenesis, *Philos. Trans. R. Soc., B.*, **237** (1952), 37–72. https://doi.org/10.1098/rstb.1952.0012
16. Y. Song, X. Tang, Stability, steady-state bifurcations, and turing patterns in a predator–prey model with herd behavior and prey-taxis, *Stud. Appl. Math.*, **139** (2017), 371–404. https://doi.org/10.1111/sapm.12165
17. S. Yan, D. Jia, T. Zhang, S. Yuan, Pattern dynamics in a diffusive predator-prey model with hunting cooperations, *Chaos Solitons Fractals*, **130** (2020), 109428. https://doi.org/10.1016/j.chaos.2019.109428
18. R. Peng, J. Shi, Non-existence of non-constant positive steady states of two Holling type-II predator-prey systems: strong interaction case, *J. Differ. Equations*, **247** (2009), 866–886. https://doi.org/10.1016/j.jde.2009.03.008
19. J. Wang, J. Wei, J. Shi, Global bifurcation analysis and pattern formation in homogeneous diffusive predator-prey systems, *J. Differ. Equations*, **260** (2016), 3495–3523. https://doi.org/10.1016/j.jde.2015.10.036

20. M. Chen, Pattern dynamics of a Lotka-Volterra model with taxis mechanism, *Appl. Math. Comput.*, **484** (2025), 129017. https://doi.org/10.1016/j.amc.2024.129017

21. R. Han, L. N. Guin, B. Dai, Cross-diffusion-driven pattern formation and selection in a modified Leslie-Gower predator-prey model with fear effect, *J. Biol. Syst.*, **28** (2020), 27–64. https://doi.org/10.1142/S0218339020500023

22. V. Tiwari, J. P. Tripathi, S. Mishra, R. K. Upadhyay, Modeling the fear effect and stability of non-equilibrium patterns in mutually interfering predator-prey systems, *Appl. Math. Comput.*, **371** (2020), 124948. https://doi.org/10.1016/j.amc.2019.124948

23. T. Zhang, T. Zhang, X. Meng, Stability analysis of a chemostat model with maintenance energy, *Appl. Math. Lett.*, **68** (2017), 1–7. https://doi.org/10.1016/j.aml.2016.12.007

24. F. Yi, J. Wei, J. Shi, Bifurcation and spatiotemporal patterns in a homogeneous diffusive predator-prey system, *J. Differ. Equations*, **246** (2009), 1944–1977. https://doi.org/10.1016/j.jde.2008.10.024

25. B. D. Hassard, N. D. Kazarinoff, Y. Wan, *Theory and Applications of Hopf Bifurcation*, Cambridge University Press, Cambridge, 1981.

26. M. Liu, E. Liz, G. Röst, Endemic bubbles generated by delayed behavioral response: Global stability and bifurcation switches in an SIS model, *SIAM J. Appl. Math.*, **75** (2015), 75–91. https://doi.org/10.1137/140972652

27. X. Wang, Y. Tan, Y. Cai, W. Wang, Impact of the fear effect on the stability and bifurcation of a leslie-gower predator-prey model, *Int. J. Bifurcation Chaos*, **30** (2020), 2050210. https://doi.org/10.1142/S0218127420502107

AIMS Press